



الجمهورية الجزائرية الديمقراطية الشعبية
People's Democratic Republic of Algeria
وزارة التعليم العالي والبحث العلمي
Ministry of Higher Education and Scientific Research



جامعة العربي التبسي - تبسة
Echahid Cheikh Larbi Tebessi University – Tebessa
معهد المناجم
Mining Institute

قسم المناجم والجيوتكنولوجيا
Department of mines and geotechnology
Presented with the aim of obtaining an academic Master's degree

Field: Mining Engineering

Option: Geotechnics

Geotechnical conditions investigation and
safety factors prediction of a new open pit
mine Gara Djibilet -Tindouf

Submitted by

BELKHIRI Anissa

Board of Examiners :

		Grade	Etablissement
Chairman:	DJELLALI Adel	MCA	Echahid Cheikh Larbi Tebessi University – Tebessa
Supervisor :	BERRAH Yacine	MCB	Echahid Cheikh Larbi Tebessi University – Tebessa
Examiner:	BRAHMI Sarhan	MAA	Echahid Cheikh Larbi Tebessi University – Tebessa

Academic Year 2022-2023





الجمهورية الجزائرية الديمقراطية الشعبية
وزارة الشهيد الشيخ التعليم العالي و البحث العلمي
جامعة العربي التبسي - تبسة



مقرر رقم: مؤرخ في: 2023/05/30

يتضمن الترخيص بمناقشة مذكرة الماستر

إن مدير جامعة العربي التبسي بتبسة،

- بموجب القرار الوزاري رقم 318 و المؤرخ في 05 ماي 2021 المتضمن تعيين السيد "قواسمية عبد الكريم" مديرا لجامعة العربي التبسي - تبسة،

- وبمقتضى المرسوم التنفيذي رقم: 12-363 مؤرخ في 8 أكتوبر 2012، يعدل و يتم المرسوم التنفيذي رقم 09 - 08 المؤرخ في: 04 جانفي 2009 و المتضمن إنشاء جامعة العربي التبسي بتبسة،

- وبمقتضى المرسوم التنفيذي رقم 08-265 المؤرخ في 17 شعبان عام 1429 الموافق 19 غشت سنة 2008 الذي يحدد نظام الدراسات للحصول على شهادة الليسانس وشهادة الماستر وشهادة الدكتوراه، لاسيما المادة 9 منه،

- وبموجب القرار رقم 362 المؤرخ في 09 جوان 2014 الذي يحدد كفايات إعداد ومناقشة مذكرة الماستر، لاسيما المادة 7 منه،

- وبموجب القرار رقم 1080 المؤرخ في 13 أكتوبر 2015 والمتضمن تأهيل ماستر الفروع ذات تسجيل وطني بجامعة تبسة.

- وبموجب القرار رقم 375 المؤرخ في 15 جوان 2020 المعدل للمحق القرار 1080 المؤرخ في 13 أكتوبر 2015 والمتضمن تأهيل ماستر الفروع ذات تسجيل وطني بجامعة تبسة، اختصاص جيوتقني

- وبموجب المقرر رقم المؤرخ في 2023/05/29 والمتضمن تعيين لجنة مناقشة مذكرة الماستر،

- وبعد الاطلاع على مقرر تعيين لجنة مناقشة مذكرة الماستر المؤرخ في

يقرر ما يأتي:

المادة الأولى: يُرخصُ للطالب (ة) بلخيري أنيسة، المولود (ة) بتاريخ 1990/07/27 ب تيزي وزو، بمناقشة مذكرة الماستر والموسومة بـ

Geotechnical conditions investigation and safety factors prediction of new open pit mine of Gara Djebilet

المادة 2: يكلف رئيس قسم المناجم والجيوتكنولوجيا بتنفيذ هذا المقرر الذي يسلم نسخة عنه إلى الطالب المعني بالمناقشة وأعضاء لجنة المناقشة فور توقيعه، وبضمان نشره عبر فضاءات المؤسسة المادية والرقمية.

المادة 3: تُحفظ نسخة عن هذا المقرر ضمن الملف البيداغوجي للطالب المعني وينشر في النشرة الرسمية لجامعة العربي التبسي.

حُزِر ب تبسة، في: 2023/05/30

عن المدير، وبتفويض منه

مدير معهد المناجم

د. عولمي زويبير
مدير معهد المناجم





مقرر رقم : مؤرخ في : 2023/05/29

يتضمن تعيين لجنة مناقشة مذكرة الماستر

إن مدير جامعة العربي التبسي بتبسة،

- بموجب القرار الوزاري رقم 318 و المؤرخ في 05 ماي 2021 المتضمن تعيين السيد "فواسمية عبد الكريم" مديرا لجامعة العربي التبسي - تبسة،

- وبمقتضى المرسوم التنفيذي رقم : 12- 363 مؤرخ في 8 أكتوبر 2012، يعدل و يتم المرسوم التنفيذي رقم 09 - 08 المؤرخ في : 04 جانفي 2009 و المتضمن إنشاء جامعة العربي التبسي بتبسة،

- وبمقتضى المرسوم التنفيذي رقم 08-265 المؤرخ في 17 شعبان عام 1429 الموافق 19 غشت سنة 2008 الذي يحدّد نظام الدراسات للحصول على شهادة الليسانس وشهادة الماستر وشهادة الدكتوراه، لاسيما المادة 9 منه،

- وبموجب القرار رقم 362 المؤرخ في 09 جوان 2014 الذي يحدّد كفاءات إعداد ومناقشة مذكرة الماستر، لاسيما المادتان 10 و 11 منه،

- وبموجب القرار رقم 1380 المؤرخ في 09 أوت 2016 والمتضمن مواءمة التكوينات في الماستر بعنوان جامعة تبسة في ميدان "علوم وتكنولوجيا".

- وبموجب القرار رقم 375 المؤرخ في 15 جوان 2020 المعدل للمحق القرار 1080 المؤرخ في 13 أكتوبر 2015 والمتضمن تأهيل ماستر الفروع ذات تسجيل وطني بجامعة تبسة، اختصاص جيوتقني

- وبعد الاطلاع على محضر المجلس العلمي لمعهد المناجم المؤرخ في.....،

يقرر ما يأتي:

المادة الأولى: تُعيّن بموجب هذا المقرر لجنة مناقشة مذكرة الماستر المحضرة من طرف الطالب (ة):

بلخيري أنيسة، المولود (ة) بتاريخ 1990/07/27 ب تيزي وزو ،

والموسومة ب Geotechnical conditions investigation and safety factors prediction of new open pit mine of Gara Djebilet

والمسجل (ة) بمعهد المناجم

المادة 2: تتشكّل اللجنة المشار إليها في المادة الأولى من الأعضاء الآتي ذكرهم:

رقم	الاسم واللقب	الرتبة	مؤسسة الانتماء	الصفة
1	جلالي عادل	أستاذ محاضر - أ	جامعة العربي التبسي - تبسة	رئيسا
2	براح ياسين	أستاذ محاضر - ب	جامعة العربي التبسي - تبسة	مشرفا
3	براهمي سرحان	أستاذ مساعد - أ	جامعة العربي التبسي - تبسة	ممتحنا

المادة 3: يكلف رئيس قسم المناجم والجيوتكنولوجيا بتنفيذ هذا المقرر الذي يُسلم نسخة عنه إلى كلّ من الطالب المعني والمشرف على المذكرة وأعضاء لجنة المناقشة فور توقيعه.

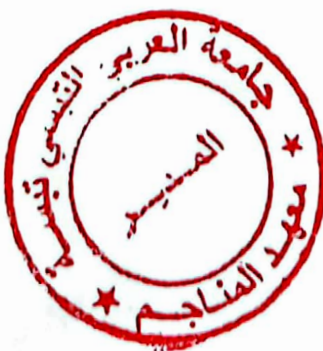
المادة 4: تحفظ نسخة عن هذا المقرر في الملفّ البيداغوجي للطالب المعني، وينشر في النشرة الرسمية لجامعة العربي التبسي.

حُزّر ب تبسة، في: 2023/05/29

عن المدير، وبتفويض منه

مدير معهد المناجم

د. عولمي زويبير
مدير معهد المناجم



Année universitaire : 2022-2023

Tébessa le : 11/06/2023

Lettre de soutenabilité

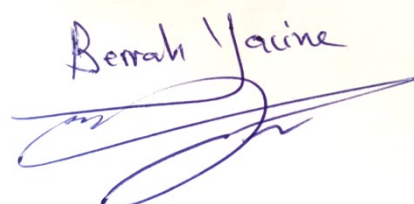
Noms et prénoms des étudiants :

BELKHIRI Anissa

Niveau : 2^{ème} **année Master** Option : Géotechnique

Thème : Geotechnical conditions investigation and safety factors prediction of a
new open pit mine Gara Djibilet -Tindouf

Nom et prénom de l'encadreur : BERRAH Yacine

Chapitres réalisés	Signature de l'encadreur
Chapiter 1 : Presentation of study area	
Chapiter 2 : Characterizing methods for rock masses	
Chapiter 3 : Geotechnical conditions investigation	
Chapiter 4 : Review on stability analysis and Safety factors prediction	
Chapiter 5: Numerical analysis of the mine stability.	

Dedication

For my success to be complete, I share it with all the people I love, I dedicate this modest work;

To my parents who today see their efforts and their sacrifices crowned by this report, They watched over my education with an infinite love and affection that I will not receive equal.

May God allow me to give them back, at least a part.

*To my brothers: Ilyas and Aymen
my sisters: Nassima, Sabiha, Souaad, Warda, Linda and Soundas.*

*To the strong Fraternal ties that unite Us.
No dedication can express my feelings to them,
I wish them much happiness and success.*

*To all the BELKHIRI family
To all my friends: Roukaya, Hadjer, djahida, Meriem, Asma
and colleagues without exception.*

*To all teachers in the mining engineering department.
To all who work with me at Khaldi A/aziz Tebessa Hospital
Especially my colleagues in the laboratory without exception.*

To all those who are dear to me.

ANISSA

Acknowledgment

I would first like to thank (الله) the almighty who gave me the health, courage and patience to carry out this work.

I thank my dear parents for their support and patience.

I express my deepest gratitude to my promoter Dr. BERRAH Yacine. for his help, his advice and his availability throughout the period of my project.

I thank Mr BOUKROUMA M (a wonderful being endowed with unparalleled skill), Mr AOUSSAT. N, Mr BELHAD. R, Dr DjELLALI. A, Mr MEBROUK. F and the whole FERAAL team for their explanations and their availability.

I would also like to warmly thank all the members of the jury for their interest in my work.

I wish to express my deep gratitude to all the teachers who trained us from primary to university.

Finally, I would like to thank all those who have directly or indirectly contributed to the realization of this work.

Abstract

The Gara Djebilet deposit in south-west Algeria is a major iron ore deposit located in the Hoggar region of the Saharan Atlas Mountains. The deposit consists of sedimentary rocks hosting iron minerals. The region is characterized by a desert environment with arid conditions and unique geological features resulting from past tectonic activity. Detailed geological studies are conducted to understand the deposit's geology, geography, and structure, aiding in determining mining methods and assessing rock mass quality. Geotechnical laboratory tests, such as the Uniaxial Compressive Strength (UCS) and Point Load Index (PLI) tests, provide essential parameters for characterizing the rock mass behavior and engineering properties. Additionally, stability analysis methods, including the finite element method and limit equilibrium method, are used to evaluate slope stability. The combination of geotechnical laboratory tests, in-situ testing, and field observations helps in comprehending the geotechnical properties of rock masses and supports rock engineering projects and slope stability analysis.

Keywords: iron ore, Gara Djebilet, geological studies, geotechnical laboratory tests, stability analysis.

Résumé

Le gisement de Gara Djebilet, dans le sud-ouest de l'Algérie, est un important gisement de minerai de fer situé dans la région du Hoggar de l'Atlas saharien. Le gisement est constitué de roches sédimentaires contenant des minéraux de fer. La région est caractérisée par un environnement désertique avec des conditions arides et des caractéristiques géologiques uniques résultant de l'activité tectonique passée. Des études géologiques détaillées sont menées pour comprendre la géologie, la géographie et la structure du gisement, ce qui permet de déterminer les méthodes d'exploitation et d'évaluer la qualité de la masse rocheuse. Les essais géotechniques en laboratoire, tels que les essais de résistance à la compression uniaxiale (UCS) et d'Indice de Charge Ponctuelle (PLI), fournissent des paramètres essentiels pour caractériser le comportement de la masse rocheuse et ses propriétés géotechniques. En outre, les méthodes d'analyse de la stabilité, y compris la méthode des éléments finis et la méthode de l'équilibre limite, sont utilisées pour évaluer la stabilité des pentes. La combinaison d'essais géotechniques en laboratoire, d'essais in situ et d'observations sur le terrain aide à comprendre les propriétés géotechniques des masses rocheuses et soutient les projets d'ingénierie des roches et l'analyse de la stabilité des pentes.

Mots clés : minerai de fer, Gara Djebilet, études géologiques, essais géotechniques en laboratoire, analyse de la stabilité..

الملخص

رواسب غارا جبيلا ت في جنوب غرب الجزائر هي رواسب خام حديد رئيسية تقع في منطقة الهقار بجبال أطلس الصحراوية. يتكون الرواسب من صخور رسوبية تحتوي على معادن حديدية . تتميز المنطقة ببيئة صحراوية ذات ظروف قاحلة وخصائص جيولوجية فريدة ناتجة عن النشاط التكتوني السابق. يتم إجراء دراسات جيولوجية مفصلة لفهم جيولوجيا وجغرافيا وهيكل الرواسب ، للمساعدة في تحديد طرق التعدين وتقييم جودة كتلة الصخور . توفر الاختبارات المعملية الجيوتقنية ، مثل اختبارات قوة الضغط أحادية المحور (UCS) ومؤشر تحميل النقاط (PLI) ، معلمات أساسية لتوصيف سلوك كتلة الصخور والخصائص الهندسية . بالإضافة إلى ذلك ، يتم استخدام طرق تحليل الثبات ، بما في ذلك طريقة العناصر المحدودة وطريقة التوازن الحدي ، لتقييم استقرار المنحدر . يساعد الجمع بين الاختبارات المعملية الجيوتقنية والاختبار في الموقع والملاحظات الميدانية في فهم الخصائص الجيوتقنية للكتل الصخرية ويدعم مشاريع هندسة الصخور وتحليل ثبات المنحدرات .

الكلمات المفتاحية : خام الحديد ، غارا جبيلا ت ، الدراسات الجيولوجية ، الاختبارات المعملية الجيوتقنية ، تحليل الثبات .

	Page
Dedication	
Acknowledgment	
Summary	
Abstract	
Notation	
List of Figures	
List of tables	
General Introduction	10
Chapter I : Presentation of study area	12
I Introduction	13
I-1 General information on Gara Djebilet iron ore	13
I-2 Location of the project host wilaya Tindouf	14
I-3 History of work carried out	15
I-4 Geographical location	16
I-5 Presentation - FERAAI, spa the national iron and steel company	17
I-6 Regional geological	19
I-7 Litho-stratigraphic overview	20
I-8 Structurally	23
I-9 General hydrogeological context	26
I-10 Climate	27
I-11 Geographical location of the Gara Djebilet deposit	28
I-11-1 Local geological	29
I-11-2 Morphology and sedimentological	32
I-12 Conclusion	35
Chapter II : Characterizing methods for rock masses	36
II Introduction	37
II-1 Rock Quality Designation (RQD):	37
II-2 Rock Mass Rating (RMR)	39
II-2-1 Estimation of the mechanical characteristics of rock masses using the RMR	43
II-2-1-a Cohesion	43
II-2-1-b The angle of friction	44
II-3 Slope Mass Rating (SMR)	44

Summary

II-4	Conclusion	48
Chapter II	Geotechnical conditions investigation	49
III-	Introduction	50
III-1	Laboratory test	50
III-2	Results of the tests carried out	51
III-2-1	Granulometric analysis (NF P94-056)	51
III-2-2	The Atterberg limits (NF P94-051)	51
III-2-3	Shear tests at the Casagrande box (NF P94-071-1)	52
III-2-4	Determination of Physical properties (density) (NF P94-053)	52
III-2-5	Compressive strength (UCS) (NF EN 12 504-1)	53
III-2-6	Direct Shear Tests	55
III-3	In addition	58
III-3-1	Density of ironstone	58
III-3-2	Ultrasonic tests	59
III-3-3	Test FRANKLIN (PLT)	60
III-4	Conclusion	62
Chapter IV:	Review on stability analysis and Safety factors prediction	63
IV	Introduction	64
IV-1	Slope stability calculation	64
IV-2	Definition of the safety factor	65
IV-3	Calculation methods	65
IV-4	Methods based on limit equilibrium (slice method)	65
IV-4-1	Method of FELLENIUS (1936)	67
IV-4-2	Simplified BISHOP method	68
IV-4-3	JANBU method (1956)	69
IV-4-4	Morgenstern and Price Method (1965)	71
IV-4-5	The differences between the methods	72
IV-5	The finite element method (FEM)	73
IV-5-1	Principle	73
IV-5-2	Discretization	73
IV-5-3	Behavioral models used in the MEF	73
IV-5-4	Calculation of the safety factor in the MEF	74
IV-6	Abacus method(Hoek's abacus)	74

Summary

IV-7	Conclusion	77
Chapter V: Numerical analysis of the mine stability		78
V	Introduction	79
V-1	The creating the geological section	80
V-2	Creating geometric models	81
V-2-1	By geo-slope code	82
V-2-1-A	Geometry model	82
V-2-1-B	Calculation	83
V-2-2	By plaxis 8.2 Code	85
V-2-2-A	Geometry model	85
V-2-2-B	Calculation and output	85
V-3	Results and conclusion	88
General conclusion		90
Bibliography		93

Notation

C	kPa	Soil cohesion
ϕ	$^{\circ}$	The internal friction angle
F_s	-	The safety factor
α	%	Slope angle
w_L	%	limit of liquidity
I_p	%	plasticity index
γ_w	Km/m ³	Water unit weight
γ_d	Km/m ³	Dry unit weight
S_r	%	Degree of saturation
FEM	-	Finite element method
LE	-	Limit Equilibrium
S	Km ²	Area
P	Km	Perimeter
H_{max}	m	Maximum altitude
L	Km	Length of main Talweg
D_s	m	Specific gradient
EC	ms/cm	The salinity of the water
S		Fracture surface
W	Km/m ³	Weight

BRGM: Bureau de recherches géologiques et minières (Geological and Mining Research Bureau).

FERAAL: Algerian national iron and steel company

IC: inclinometer.

JRC: Joint Roughness Coefficient.

MEF: Finite Element Method.

RMR: Rock Mass Rating

RQD: Rock Quality Designation

SACSIR: South African Council of Scientific and Industrial Research.

SMR: Slope Mass Rating

SONAREM: Société Nationale de Recherche et d'Exploitation Minières.

LCTP Central Laboratory of Public Works

ITU Istanbul technical university

STRX Triaxial - Consolidated undrained (CU)

HTRX Triaxial - Hoek rock triaxial (3 stage)

Notation

UCS	Unconfined compressive strength with Modulus and Poisson's ratio
DSTJ	Direct shear test (natural parting)
DSTW	Direct shear test (weak rock, $\leq R_2$; intact core)
Saw Cut	Direct shear test ($>R_2$ core; core cut by lab for basic friction)
PLT	Point Load Test (Axial and Diametral)
ATT	Atterberg limits
FOND	Ironstone (Non-Detrital Facies)
FOC	Ironstone (Cemented Facies)
FOD	Ironstone (Detrital Facies)
CG	Conglomerate
SS	Sandstone
SH	Shale
ST	Siltstone
MS	Mudstone
CS	Claystone
BR	Breccia
QS	Quaternary Sediments
OT	Other

Figures list:

Figures list:

Fig 1	Situation of the wilaya of Tindouf	15
Fig 2	Geographical location of the Gara Djebilet deposit.	17
Fig 3	Photo of FERAAL society	19
Fig 4	Photo of the Gara Djebilet Deposit	19
Fig 5	Geological map of southwestern Algeria Tindouf basin	20
Fig 6	Lithostratigraphy of the Tindouf basin	22
Fig 7	Structural map of the study area	25
Fig 8	Global linear map of the Tindouf basin in th 1/2000000th	26
Fig9	Schematic map showing the distribution of the different aquifers of the Tindouf basin	27
Fig 10	Graphic climatic of Tindouf	28
Fig 11	Location of the Gara Djebilet iron ore deposit (Google Earth)	29
Fig 12	Topographic map of the Gara Djebilet region	29
Fig 13	Geological map of the Gara-Djebilet region	31
Fig 14	Geological map of the Gara-Djebilet	32
Fig 15	Lithostratigraphic columns of the Gara Djebilet deposit	33
Fig 16	Map of Gara Djebilet facies	34
Fig 17	An example of RQD classification	37
Fig 18	Photos of drill core SA-007	38
Fig 19	RMR characterisation parameters	40
Fig 20	Orientation of a flat slope.	45
Fig 21	Particle size curve ZK08/0.2-0.7 (Fine-grained sandstone)	51
Fig 22	Curve of Atterberg limits ZK08/0.2-0.7	51
Fig 23	Stress – strain graph for ZK02	54
Fig 24	Stress – strain graph for ZK03	54
Fig 25	Shear stress-strain graph for ZK-8 and ZK-3	56
Fig 26	Shear and normal stress graph for ZK-8 and ZK-3	57
Fig 27	Uniaxial Compressive Strength Sample ZK03 A (Before) B (After)	57
Fig 28	Photo of realization the density of ironstone	58
Fig 29	Photos of realization ultrasonic test of ironstone	54
Fig 30	Photos of realization test point load	61
Fig 31	Description of the failure surface	64

Figures list:

Fig 32	Description of slicing with breaking surface	66
Fig 33	Demonstration of forces acting on a wafer.	66
Fig 34	Forces acting on a surface according to FELLENIUS	67
Fig 35	Forces considered in Janbu's method	69
Fig 36	Variation of the correction factor according to depth and length of the fracture surface	70
Fig 37	Representation of forces on a slice using the simplified method of Morgenstern and Price.	72
Fig 38	Hoek chart for calculating the safety factor (Fs)	76
Fig 39	Cross section geological	81
Fig 40	Geometry of model 1	82
Fig 41	Geometry of model 2	83
Fig 42	Failure area and value of Fs model 1	83
Fig 43	Failure area and value of Fs model 2	84
Fig 44	Model geometry (code plaxis 8.2)	85
Fig 45	Displacement total	85
Fig 46	Relative shear stresses	85
Fig 47	Shear-strains	86
Fig 48	Value of the safety factor before exploitation	86
Fig 49	Value of the safety factor After exploitation	87

Tables list

Tables list:

Table I-1	Typical stratigraphic litho column of the Tindouf basin	21
Table I-2	Table summarizing all the tectonic events and sedimentary at the level of the platt Saharan form during the Paleozoic.	24
Table II-1	The RQD index and the quality of the rock mass.	38
Table II-2	Value of the RQD	39
Table II-3	RMR classification (Bieniawski, 1989)	41
Table II-4	Classification of rock mass according to RMR; adapted from Bieniawski.	41
Table II-5	Value of the RMR	42
Table II-6	Value of the cohesion	43
Table II-7	Value of the angle of friction	44
Table II-8	Romana classification.	46
Table II-9	The different stability classes by SMR value	47
Table II-10	SMR values	47
Table III-1	Value of the Atterberg limits	51
Table III-2	Value of the cohesion and Angle of internal friction in degree	52
Table III-3	Physical properties test results	52
Table III-4	Value of the uniaxial compressive strength	53
Table III-5	Value of the young's module and poison ration	53
Table III-6	Direct shear test results for DSTJ & DSTW	55
Table III-7	Value density of ironstone	58
Table III-8	Value poison coefficient and young's modulus of ironstone	60
Table III-9	Value de PLT and resistance of compression under point load	61
Table IV-1	Consideration of the balance of forces and moments according to the different methods.	72
Table IV-2	Consideration of the vertical and horizontal inter-slice forces according to the different methods.	72
Table V-1	Geotechnical parameters of the layers	82

General

Introduction

General Introduction

Mining plays a significant role in the economy of Algeria. The country is known for its significant reserves of iron ore, phosphate, lead, zinc, mercury, and uranium, among others. These resources serve as a foundation for the mining industry and contribute to the country's economic development. Stability in mines especially in an open pit mine refers to the ability of the mine walls or slopes to maintain their integrity and resist failure. It is crucial to ensure stability to protect the safety of personnel, equipment, and infrastructure within the mine.

Stability in an open pit mine refers to the ability of the mine walls or slopes to maintain their integrity and resist failure. It is crucial to ensure stability to protect the safety of personnel, equipment, and infrastructure within the mine. One of the most important key factors and measures that contribute to stability in an open pit mine is the geotechnical conditions analysis, thorough this analysis conducted to assess the geological and geotechnical properties of the rock and soil materials present in the mine helps determine the potential stability issues and design appropriate slope angles.

This final memory project presents a geotechnical study and safety factor prediction and estimation for the GaraDjebilet iron ore mine, and it aims to address the issue of preventive stability by carrying out a characterization study of the rock mass, also by using simulation software.

The total project work is composed of five chapters as follows:

The first chapter describes the geographical and geological setting of the study site, detailing their structural and stratigraphic characteristics.

The second chapter illustrate the RQD (Rock Quality Designation) and RMR (Rock Mass Rating) classification systems applied to the mine rock mass and assesses its stability using the semi-empirical SMR (Stability Matrix Rating) system.

The third chapter deals with the long-term stability of slopes during mining operations and rock weathering. Stability calculations carried out to predict long-term slope stability.

General Introduction

The fourth chapter examines the methods used to assess the stability of slopes and mining structures, as well as the various methods for determining the factor of safety.

The fifth chapter presents the simulation and some predictive scenarios of the mine's stability using Plaxis 8.2 and Géo-Slope software.

CHAPTER

1

I- Introduction

The geographical and geological situation of a region can play a crucial role in the development of the mining industry. In the specific case of the Gara Djebilet iron ore mine, it is important to understand the region in which it is located and the importance of its operation.

Gara Djebilet is an iron ore mine located in the Tindouf region of Algeria, close to the border with Mauritania. The Tindouf region is characterised by a desert environment, with stretches of sand and mountainous terrain. The area is known for its vast reserves of high-quality iron ore.

The importance of the Gara Djebilet iron mine lies in its abundant mineral resources. Iron ore is an essential raw material in the production of steel, which is used in many industrial sectors, such as construction, automotive and equipment manufacturing. Global demand for iron ore is high, and mines like Gara Djebilet are helping to meet this growing demand.

The Gara Djebilet mine offers significant economic benefits for the region and the country. It generates income, creates jobs and promotes the development of local infrastructure. In addition, the mining industry can stimulate economic growth by promoting the development of ancillary services such as transport, logistics and construction.

However, it is important to note that mining can also pose environmental and social challenges. Protection of the environment, responsible management of natural resources and mitigation of negative impacts on local communities are crucial aspects to consider when operating the Gara Djebilet iron ore mine, in order to ensure sustainable and balanced development.

I-1 General information on Gara Djebilet iron ore

On March 19, 2021, Algeria signed a memorandum of understanding with China's CITIC Construction for the construction of the Gara Djebilet iron mine and a steel complex. The project is expected to cost around \$5 billion and will be jointly owned by the Algerian government and CITIC Construction. The project aims to produce 10 million tons of iron per year and 1 million iron mine. The agreement includes the construction of a mine, a railway line of 600 km to transport the iron ore to the Mediterranean coast, and a

deep-water port. The project is estimated to cost \$6.2 billion and is expected to be completed in five years.

The Gara Djebilet iron deposit is considered a strategic national resource for Algeria, as the country seeks to diversify its economy away from dependence on oil and gas. The project is expected to generate significant revenue for Algeria and create employment opportunities for its citizens.

However, the project has faced opposition from local populations and environmental groups, who argue that it will have a negative impact on the environment and the livelihoods of local communities. They are concerned about the potential destruction of natural habitats, water resources, and the displacement of pastoral communities who rely on the area for their livelihoods.

In response to these concerns, the Algerian government has pledged to carry out an environmental impact assessment and implement measures to mitigate the impact of the project on the environment and local communities. It remains to be seen how these concerns will be addressed and whether the project will proceed as planned. [1;2]

I-2 Location of the project host wilaya Tindouf

The wilaya of Tindouf was created under the administrative division of 1984; it is located in the extreme South-West, limited as follows:

- To the North by the Kingdom of Morocco.
- To the North-East by the wilaya of Bechar.
- In the South by the Mauritanian Islamic Republic.
- In the North-West by the Saharawi Republic.
- To the east by the wilaya of Adrar.

The geographical coordinates of the wilaya of Tindouf are:

- Longitude: $x_1 = -8.500000000^\circ$, $x_2 = -2.979209001^\circ$
- Latitude: $y_1 = 25.51272200^\circ$, $y_2 = 29.61417200^\circ$. [3]

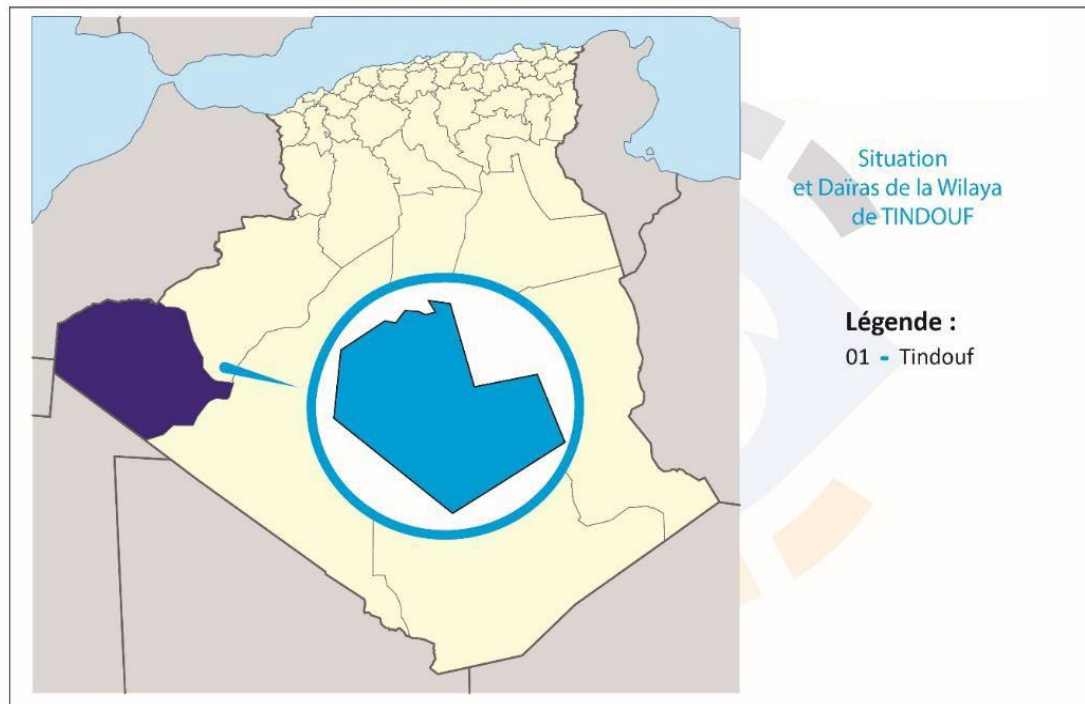


Fig 1: Situation of the wilaya of Tindouf [3]

I-3History of work carried out

1- 1952: P.Gevin: discovered the deposit during a geological survey of the region.

2- 1953-1.954: the BRMA began prospecting for the deposit: 32 wells and 34 boreholes implanted according to a triangular mesh of 500 m side volume 1100 m) were executed at

Gara Centre, 15 wells at Gara west and 5 boreholes at Gara East. Magnetic prospecting on the ground was also carried out.

During this stage, J.Y. The bault and M. Bourgeois undertook a geological study punctuated by a geological sketch at 1/100,000

3- 1957: the BIA (Office of Mining Research) carried out a program of 118 drillings coring performed at Gara Center i.e. one with a volume of 4950 m,

4- 1960: SERMI continued work at Gara west by carrying out 51 boreholes and 3wells showing significant reserves, The total drilling volume exceeded 7000m.In the light of the results obtained, studies have been undertaken on the exploitation of the ore and its evacuation.

5- 1962: a test station was built near Gara west allowingto study the possibilities of enrichment of the ore by dry destoning on separatorslow intensity magnets.

6- 1967: FRIED KRUPP ROHSTOFFE carried out a study on the use of ore of iron.

7-1976/78: IDROTECHNECO carried out on behalf of SONAREM (research and mining company) a hydrogeological study of the Tindouf region.

8-1980; KAISER (kaiser Engineers and Constructors Inc.) conducted a feasibility study exploitation of the Gara-Djebilet deposit.

9- Other foreign partners have carried out studies on the Gara-Djebilet deposit and MecheriAbdelaziz in particular: LKAB (Sweden), IRSID (France), KLOCNER GRÀ), NSEJapan). The purpose of these studies was to seek an increase in iron anda decrease in the levels of harmful elements (phosphorus and arsenic)

10- From 2013-2014, following a conclusive study (decrease in the levels of harmful elements - Phosphorus and Arsenic) a tight-mesh core drilling campaign is launched on Gara west, aims to study the feasibility of operating the mine.

2.11- completed in 2016: Topographic survey and geological survey at 1/5000 of the first part of Gara west area 6000 Ha. [4; 5]

I-4 Geographical location

The Gara Djebilet iron deposit is located in Western Sahara Algerian, approximately 135 km southeast of Tindouf. The deposit takes its name from the location where it is situated. The area has a slightly hilly terrain with altitudes ranging between 400-500m, and a continental (Saharan) climate characterized by hot, dry summers and mild, cool winters. Rainfall is minimal, averaging only 1.00 mm/year, and sandstorms can be frequent and strong, particularly in the spring. The fauna and flora in the region are rare and typical of Saharan regions. The local population has relocated to the chief town of the wilaya for social and economic reasons. The area has basic infrastructure, including an administrative branch, a health center, electricity, and drinking water provided through a survey. [6; 7; 8]

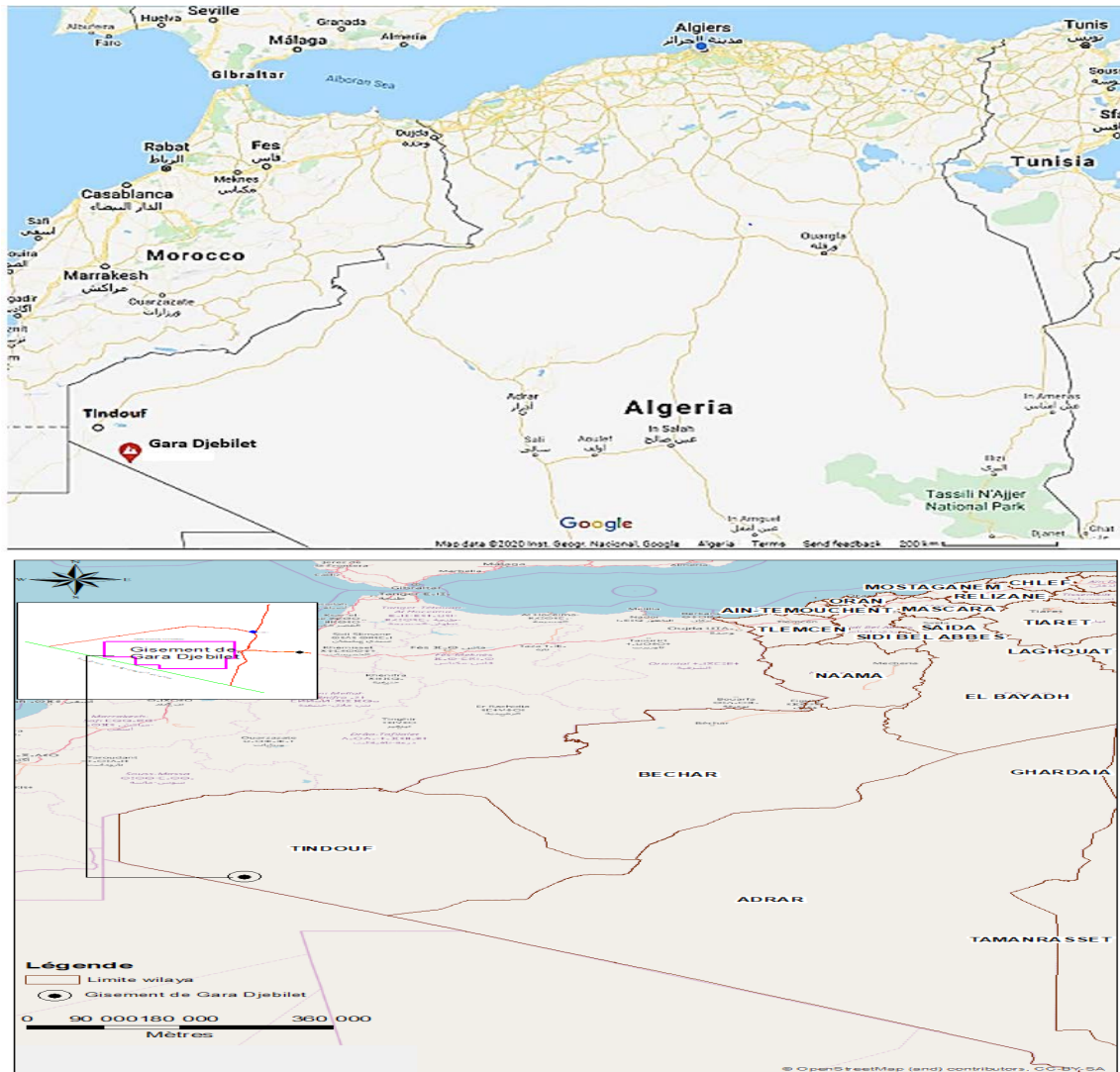


Fig 2: Geographical location of the Gara Djebilet deposit.

This open-pit mine whose myth associated with the El Dorado of inexhaustible wealth has rocked generations of Algerians. It has been recognized by more than 200 core drillings totaling 7,000 meters. Its exploitable reserves are around 1.7 billion tons at 57% iron, located in two important lenses: a so-called "west" lens with 780 million tons and a so-called "center" lens with 900 million tons. [3]

I-5 Presentation - FERAAL, SPA the national iron and steel company

- The exploitation of the iron deposit
- Extraction and preparation of various mineral products
- The operation of the mine



- iron ore processing

-Medium dephosphorus ore, pellet (a ore conditioning) or iron powder pre-reduced

(PDR)

Nature: Seat

Year of creation: 2014

Legal form SPA

Capital: 1,000,000,000 DZD

Company workforce From : 20 to 49 employees

ACTIVITIES

Drawn, compressed and turned irons and steels. Hollow round and square steels

- Hot drawn steel semi-finished products

Rolling of metal parts

- Upsetting iron and steel

Boilermaking

- Iron and cast iron boilermaking

Installation and maintenance of railway equipment

- Turning railroad wheels

Commodity Brokers, Futures Trading

- Brokers in metals, minerals and ores

Engineering consultancy for transport infrastructure and traffic

- Engineering consultancy for railway signaling and safety systems. [9]



Fig 3: Photo of FERAAL society

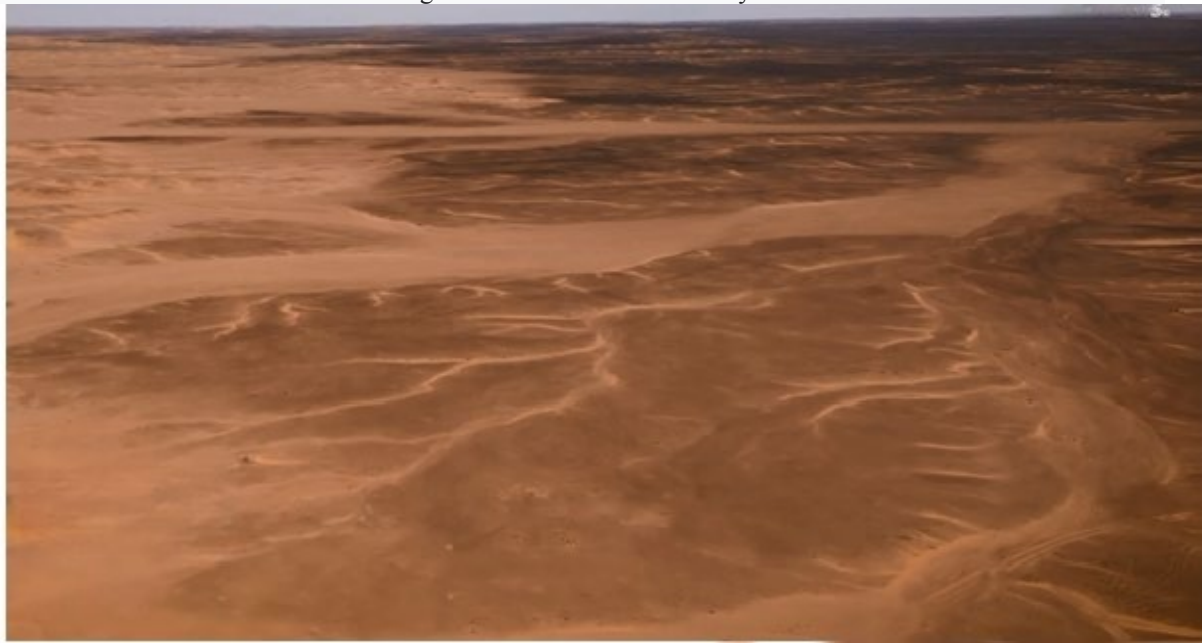


Fig 4: Photo of the Gara Djebilet Deposit

I-6 Regional geological

The Tindouf basin's geology varies from north to south, with the northern side exhibiting a deformed Paleozoic series with abundant dolerite injections, while the southern side shows less deformation, where the Paleozoic series rests unconformably on the Precambrian basement of the Reguibat ridge (as shown in Figure 5). The rocks found within the Tindouf region belong to two distinct structural units with different ages, which are the Yetti-Eglab massif and the Tindouf basin. The Tindouf basin is an elongated asymmetrical depression that stretches approximately 800 km long by 200 to 400 km wide,

with a slightly inclined southern flank and a much straightened northern flank. It is bounded by the Anti-Atlas to the north, the Reguibat ridge to the south, the Ougarta chains and the Reggane depression to the east, and the El Aioun basin and the Mauritanides to the west. The sedimentary cover within the basin thickens regularly, from around 1500m in the south to 8000m in the north. The central part of the basin is obscured by Cretaceous and Tertiary "Hamadian" continental formations. [10; 11;]

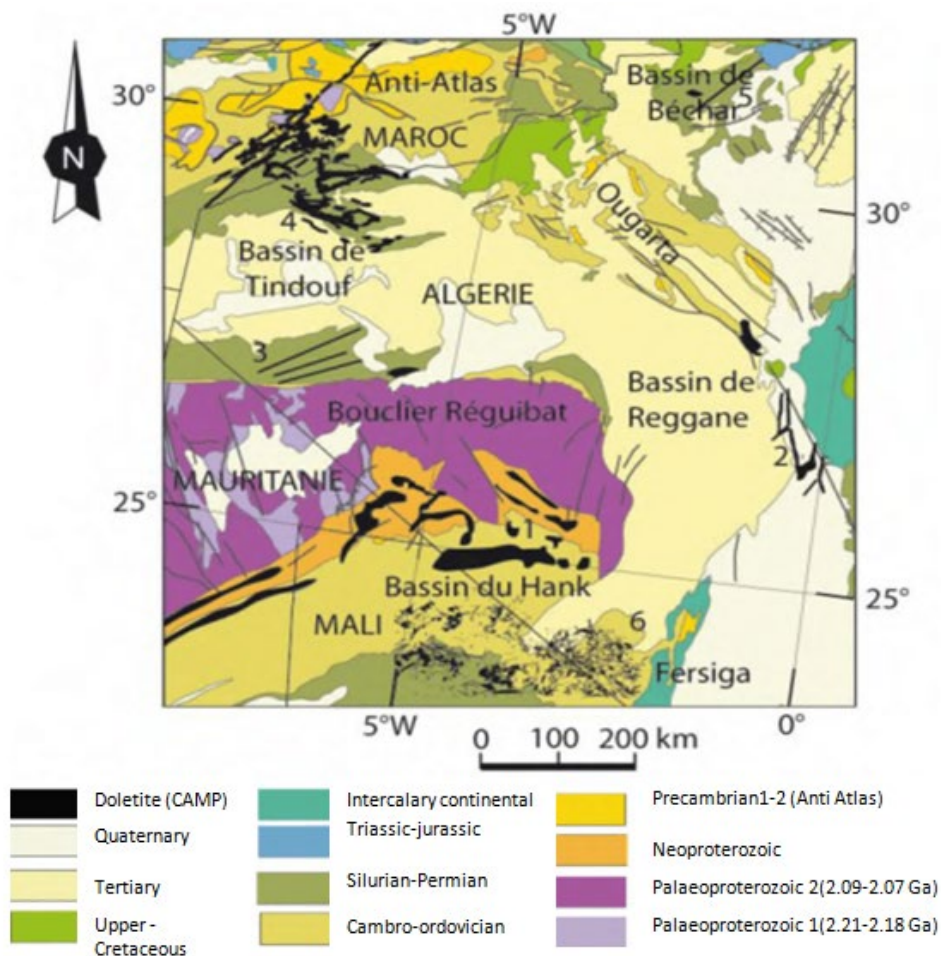


Fig 5: Geological map of southwestern Algeria Tindouf basin. (From the geological map of Africa at 1/10,000,000, BRGM 2004) [12]

I-7 Litho-stratigraphic overview

The basin is filled with sedimentary deposits from the Paleozoic, Meso-Cenozoic, and Quaternary periods. These formations rest on an uneven base in a significant unconformity. A type stratigraphic column summarizing these formations is presented in Table I-1 and Fig 6. The sedimentary deposits are mostly limited in size.

Table I-1: Typical stratigraphic litho column of the Tindouf basin [13; 14]

Echelle Stratigraphique		Bassin de Tindouf		DEVONNIEN	Inferieur	Emsien	Grès supra-minéraux	Grès du 2ème Rich
		Sud	Nord			Praguien Lochkovien	Grès de Djebilet	Argiles et calcaires du 1er Rich
PERMIEN (Autunien)				SILURIEN	Superieur	Pridolien Ludlowien	Argiles de la Sebkha Mabbes	Argiles à Graptolites
						Wenlockien Llandovérien		
CARBONIFERE	Superieur	Stépahalien		ORDOVICIEN	Superieur	Ashgillien	Grès de Rhezziand	Grès du 2ème Bani
		Westphalien (Moscovien)				Caradocien		Grès de Rouid Aïssa Schistes de Ktaoua Grès du 1ème Bani
		Namurien				Llandeiniien	Argiles d'Aroueta	Argiles de Tachilla
	Inferieur	Viséen		Inferieur	Llanvirnien	Schistes des Feija externes Grès de Zamzouata supérieurs Schistes de Fazouata inférieurs		
		Tournaisien			Arénigien			
					Trémadocien			
DEVONNIEN	Superieur	Strunien	Grès de Kerb En Naga	CAMBRIEN	Supérieur	Grès d'Aroueta supérieurs	Grès à Lingules Schistes à Paradoxides	
		Famennien	Argiles de l'Oued Slouguia		Inferieur		Grès d'Aroueta inférieur	Grès terminaux Schistes de base Grès de Tiktj Calcaires à Archeogyathidés Groupe de Jata (Adoudoumien)
	Moyen	Frasnien	Siltites de l'Oued Rhazzal	NEOPROTEROZOÏQUE				Groupe de Ouarzazate (PII) (Série volcano-détritique et argilo-gréseuse rouge) Groupe de Saghro (PII-III) (Série volcano-détritique)
		Givétien	Calcaire de la Kerba Tsabia					Calcaires à Ptéropodes
		Eifélien (Couvinién)	Argiles de l'Oued Talha					Argiles à Ptéropodes
				PALEOPROTEZOÏQUE		SOCLE DE REGUIBAT (EBURNEEN)		

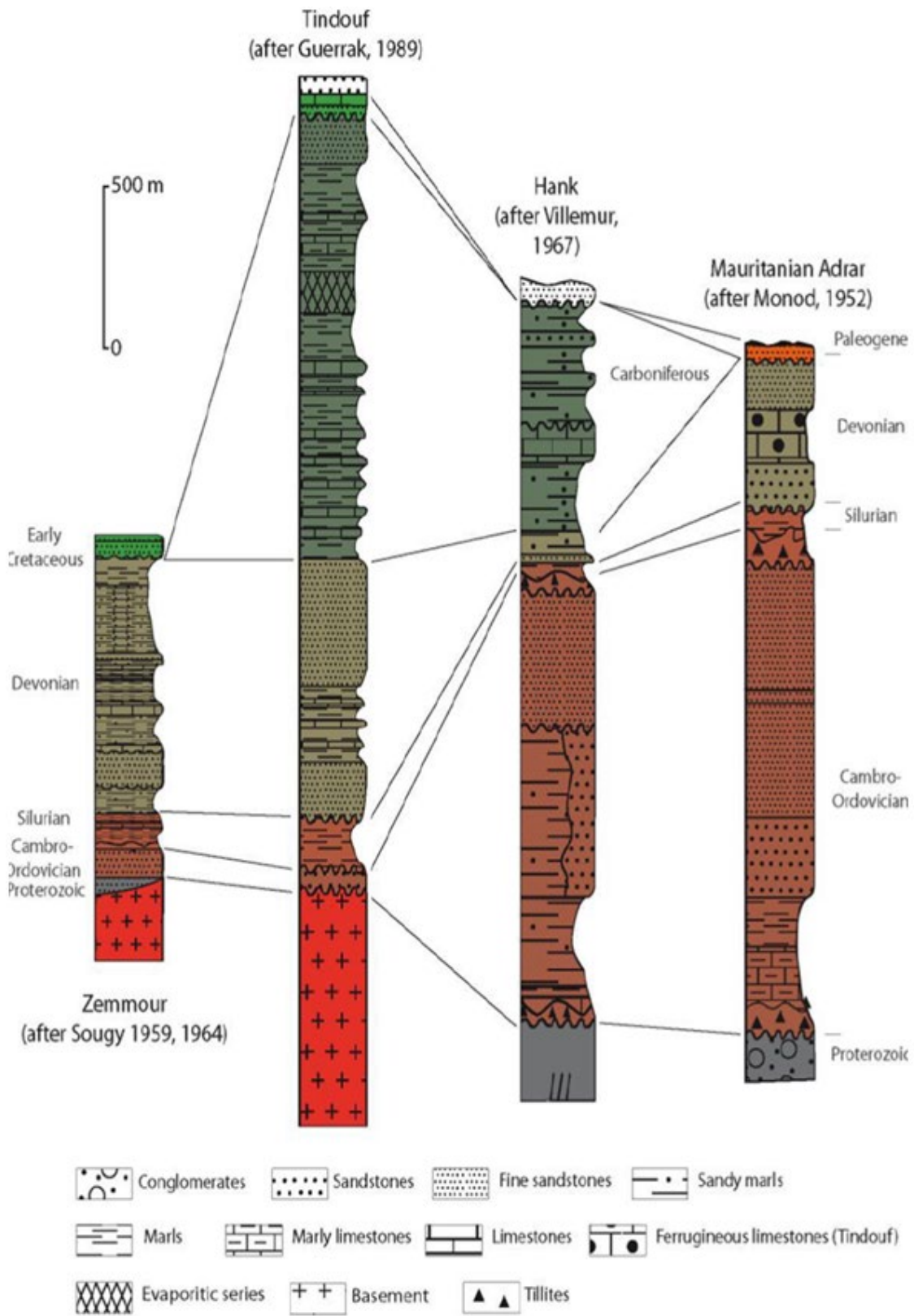


Fig 6: Lithostratigraphy of the Tindouf basin. [13]

I-8 Structurally

The Tindouf basin has a long history, beginning from the Precambrian and functioning during the Paleozoic. It has undergone intense tectonic phases over time, resulting in its current structure on the Saharan platform. These phases are summarized in Table 2. The Pan-African cycle, characterized by the reactivation of major meridian accidents of plinth with bulges parallel to the Pan-African suture, was followed by the Caledonian cycle. During this phase, up-lifts occurred in the Tindouf basin, with distinct sub-basins separated by oblique faults. The Hercynian cycle caused significant epirogenic activity, generating large folds with radii of curvature and oblique faults. The alpine cycle followed, taking over the old structures and resulting in post-Hercynian and post-Hamadian movements. The post-Hercynian phase was a period of relaxation that ended with extensive tectonics, while the post-Hamadian movements resumed the Paleozoic curvatures underlying and the ultimate Hercynian fractures.[15; 16]

Table 2: Table summarizing all the tectonic events and sedimentary at the level of the platt Saharan form during the Paleozoic.

Period	Tectonic phases	Rift	Influence on sedimentation
Barremian	Austrian	Normal Rifts N-S & NE-SW	Erosion of Lais sediments in the Cretaceous
Traissic-Liassic	Rifting	Reverse Rifts NE-SW	Erosion on the axes NE-SW
EarlyCarboniferousVisean	EarlyHercynian	Reverse RiftsNE- SW	Erosion on the axes NE-SW
Dévonien	////////////////////	////////////////////	Non-deposition and local erosion (Mol d'ahara)
Siluro-Dévonian	Ardennes	Reverse Rifts N-S	Erosion on the submeridian moles
Ordovician-Silurian	Taconic	Reverse Rifts N-S	Uprising of the Tuareg shield and Réguibat
Cambro-Ordovician	Sardinian	Normal Rifts N-S	Variation of thicknesses controlled by Rifts and Volcanism
Cambrian	Late Pan-African	Rifts NE-SW & NW-SE	Cratonization of central sahara

The sedimentary cover of the Tindouf basin underwent several tectonic phases, with major NE-SW and ENE-WSW trending faults cutting across the region, linked to magmatic rises of gabbro-dolerites, a calendar of phases of deformation of the basin was established, which includes the following forms of dolerites: dykes, sills, and intrusive massifs. Dykes are the most widespread type of structure in this region and are generally thin (1 to 10 m) with a triple bundle orientation. Sills are rare and thin in this part of the basin, while intrusive massifs, probably "chimneys," are also known in the region and affect large areas. The age of the dolerites is later than the Upper Carboniferous, likely Mesozoic. [17; 18]

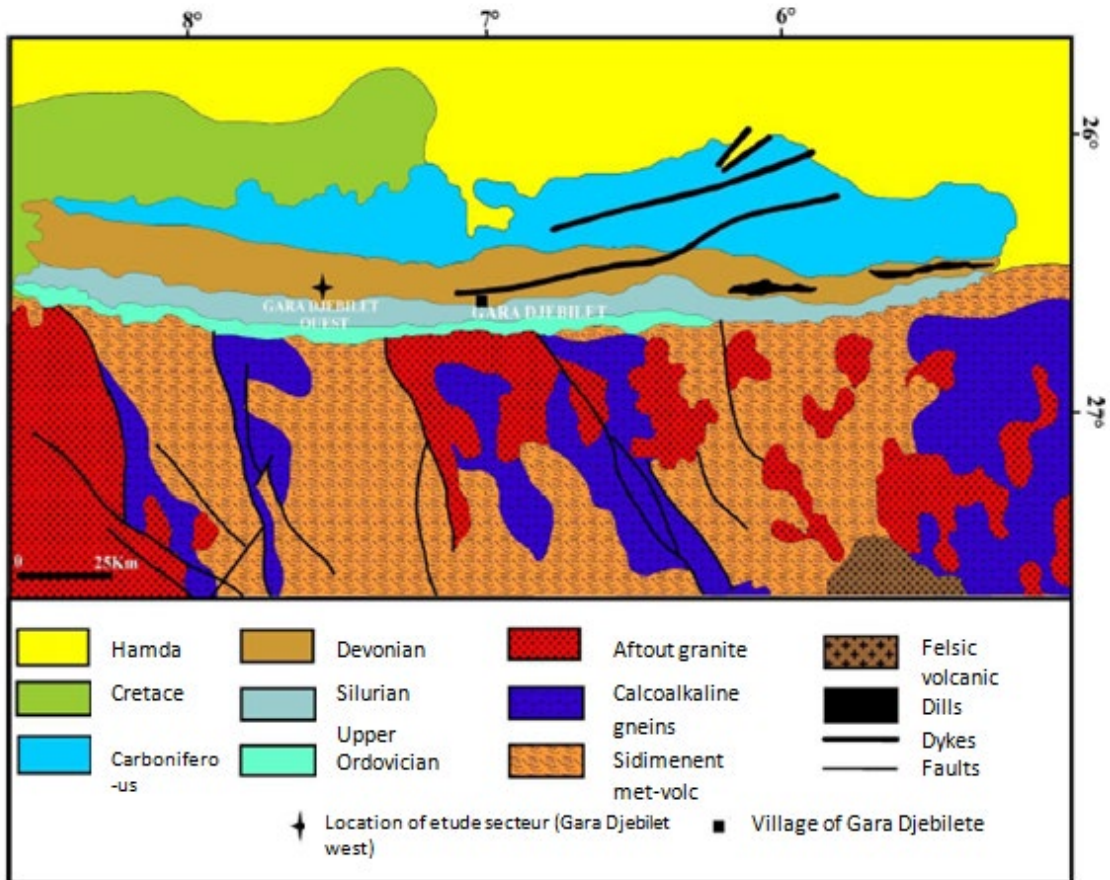


Fig 7: Structural map of the study area [19; 20]

Hercynian tectonics is the phase having structured the basin.

The analysis of the map of the major lineaments of the basin (fig 8) shows the combination of several directions.

- The NE-SW and NW-SE directions, linked to the presence of dolerites, seem to be the most important and most common.
- The E-W direction is located mainly in the north of the basin in the Zémoul region.
- The N-S direction is concentrated on the NE edge of the Eglabs massif. [21]

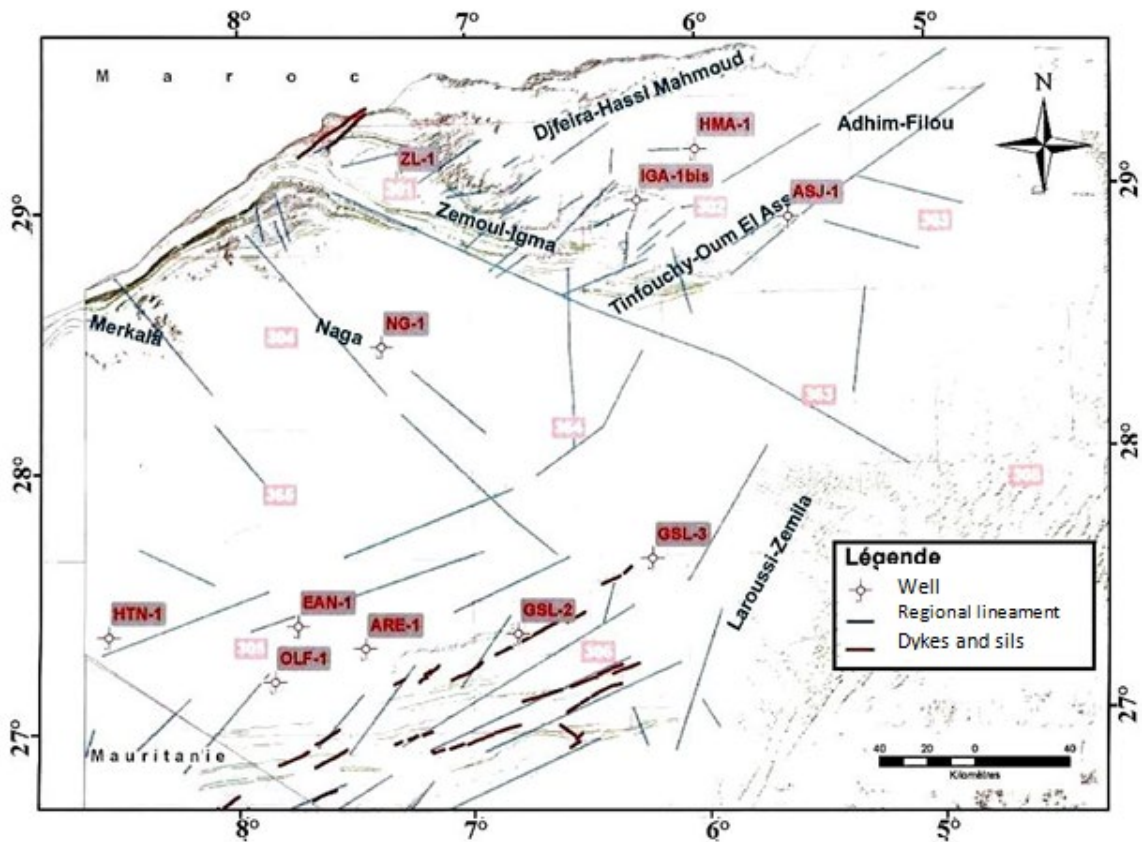


Fig 8: Global linear map of the Tindouf basin in th 1/2000000th. [20]

I-9 General hydrogeological context

Studies conducted on the Tindouf basin's various structural stages have revealed a Precambrian crystalline base consisting of schists, quartzites, and granite rocks. This crystalline basement is overlain by a sedimentary cover in angular discordance, forming an extensive syncline structure. The foundation of this structure comprises primarily Paleozoic deposits, overlaid by the Hamadian formations attributed to the Tertiary and Quaternary periods. The aquifers in the Tindouf basin are arranged from bottom to top. [22]

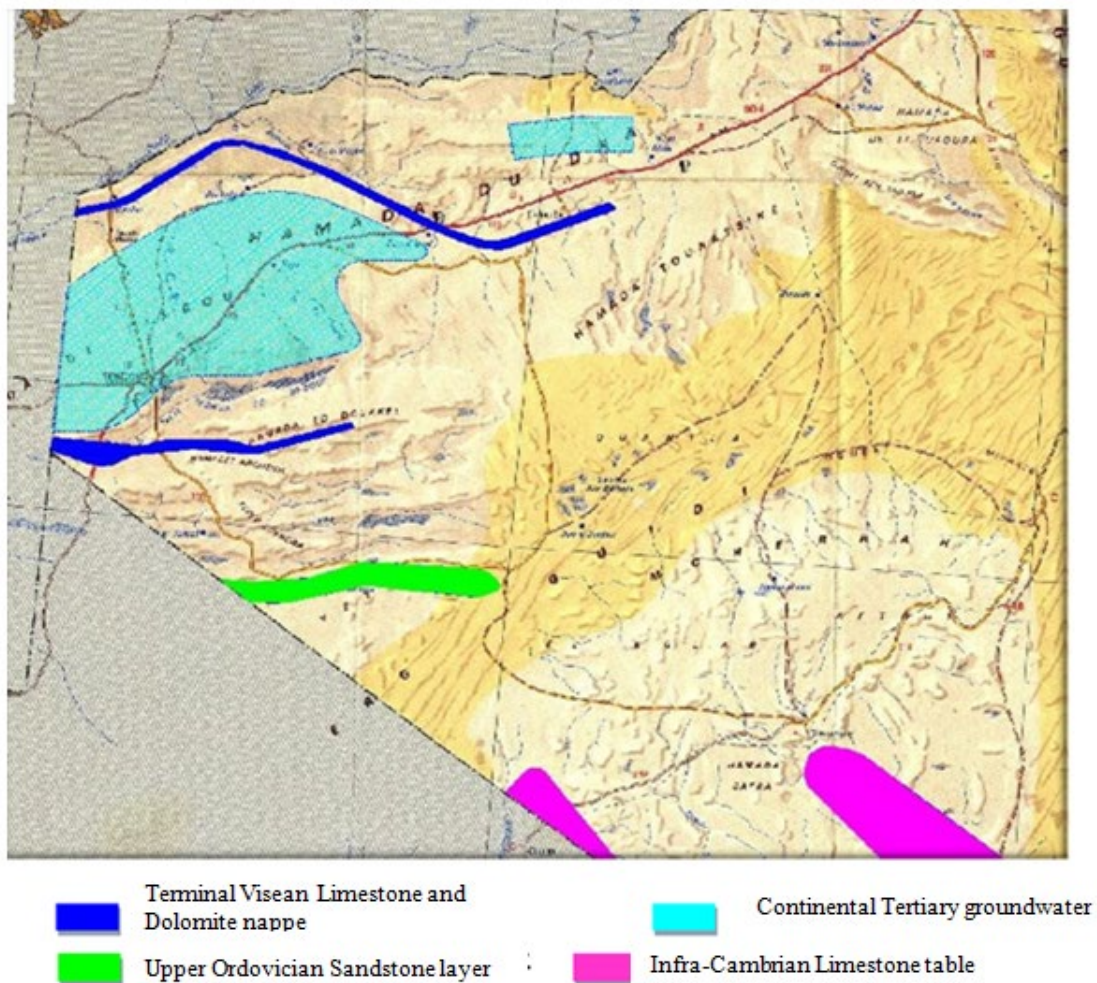


Fig 9: Schematic map showing the distribution of the different aquifers of the Tindouf basin [23]

I-10 Climate

The climate refers to a range of phenomena such as wind, precipitation, temperature, and evaporation that differ from one location to another on the earth's surface. The climatology of the Sahara is a complicated area of study due to the limited amount of precipitation and the sparse distribution of meteorological stations in the region. The climate of Tindouf is subtropical desert, with very mild winters (but during which it can be cold at night) and very hot and sunny summers (fig 11). [24]

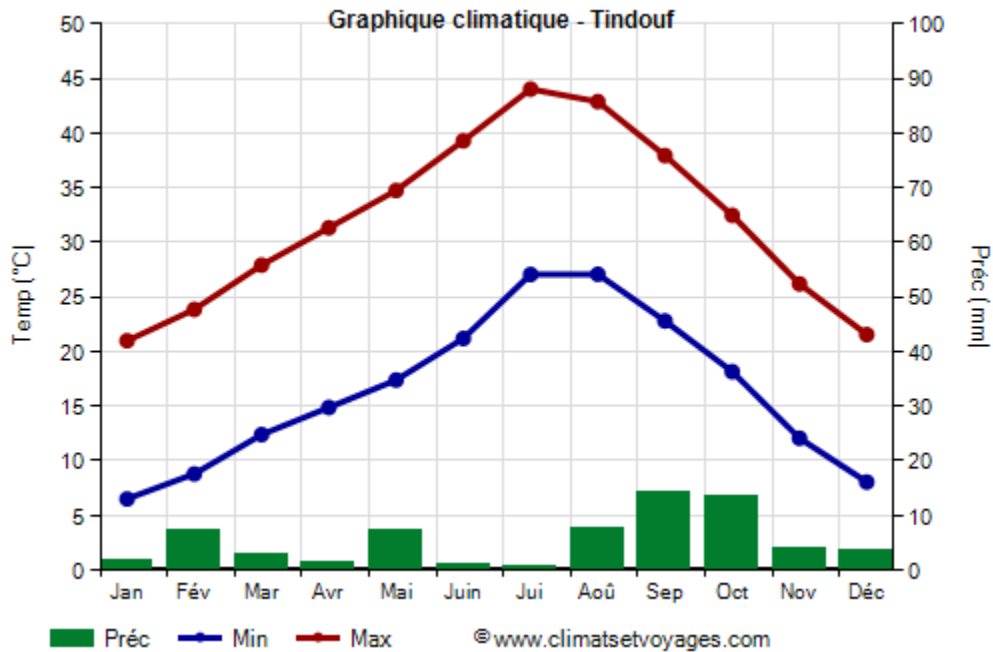


Fig 10: Graphic climatic of Tindouf [25]

I-11 Geographical location of the Gara Djebilet deposit

The Gara Djebilet iron ore deposit is located in southwestern Algeria. It is located 130 km southeast of the town of Tindouf, near the Algerian-Mauritanian border, 300 km as the crow flies from the Atlantic Ocean and 1,600 km south of the Algerian coast.

The iron deposit – Gara Djebilet - whose name is borrowed from the locality where it lies, is located about 135 km, south-east (SE) of Tindouf (chief town of the wilaya) in the Algerian Western Sahara. The main road linking the two localities (Tindouf and Gara Djebilet) is paved. The relief is slightly hilly, the altitudes oscillate between 400-500m.

Southwest corner of the country:

26°44'47"N

7°15'47"W



Fig 11: Location of the Gara Djebilet iron ore deposit (Google Earth)

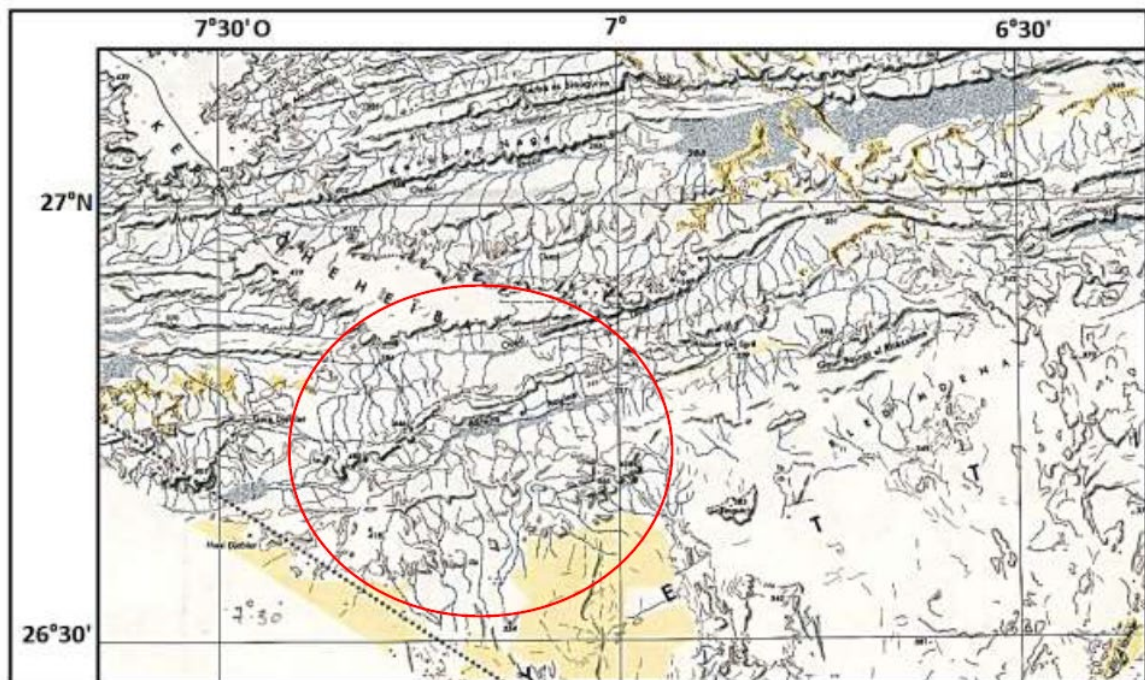


Fig 12: Topographic map of the Gara Djebilet region (Excerpt from the topographic map of Tinduf NG-29 N-E, 1/500000)

I-11-1 Local geological

The Gara Djebilet iron deposit is located in the Lower Devonian formations of the S flank of the Tindouf syncline, at a distance of about 135 km SW of this agglomeration. The

primary series that make up this region have a very slight dip towards the N, and lie unconformably on the precambrian basement, which outcrops more to the S in the form of the granitic massif of Yetty. These are sedimentary series of generally variable power, but having undergone almost no tectonic manifestation. The most salient feature of the local topography is the existence of a large cliff, looking towards the S, whose upper part is constituted by the ore itself, and which gradually lowers towards the E, to disappear at the NE end of the central Gara.

The following formations were successively deposited on the precambrian basement:

1. Cambro-Ordovician. Coarse sandstone. Their power, minimum between the two Gara (5m), increases rapidly towards the W and towards the E (100 m at AouinetLegraa).
2. Gothlandian. Shale and fine sandstone. Their power decreases from W to E (transgression towards E)
3. Gedinian and Sigenician. The series includes two terms from bottom to top:
 - Schists and fine laminated sandstones with a ferruginous oolitic level which provides a good stratigraphic reference.
 - Sandstone-schistose series surmounted by a bench of ocher sandstone, coarse, with intersecting stratification, taking towards the E where they rest in discordance on the preceding terms, a clearly transgressive pace. Above, clays and sandstone of the wall.
4. Emsien.
 - The base is none other than the main bench of oolitic ore surmounted by the "roof ore" presenting clay intercalations of cylindrical shape, possibly corresponding to old plant stems. The ore of the roof becomes more and more conglomeratic towards the S, and takes on a transgressive aspect.
 - Fine sandstone and ferruginous quartzites. This is the term for the lateral passage of the ore, to the E and W of the Garas. The transition is generally very abrupt as if there had been a very rapid modification in space of the conditions of sedimentation. It is accompanied by a decrease in potency.
 - Sandstone and sandstone limestone with *Spriferia pellicoi*. They constitute the roof of the ore in the West Gara, extend between the two Garas but disappear in the Central Gara and reappear more to the E.
 - Thin slab of purplish limestone with Crinoid articles, absent at the Central Gara.

5. Eifelian.

- Pink sandstone with *Spirifer cultrijugatus*.
- Ferruginous quartzites with a brilliant luster
- Clays and marls with *Spirifer speciosus* and past shell limestone
- Limestone bench with polypies.[27]

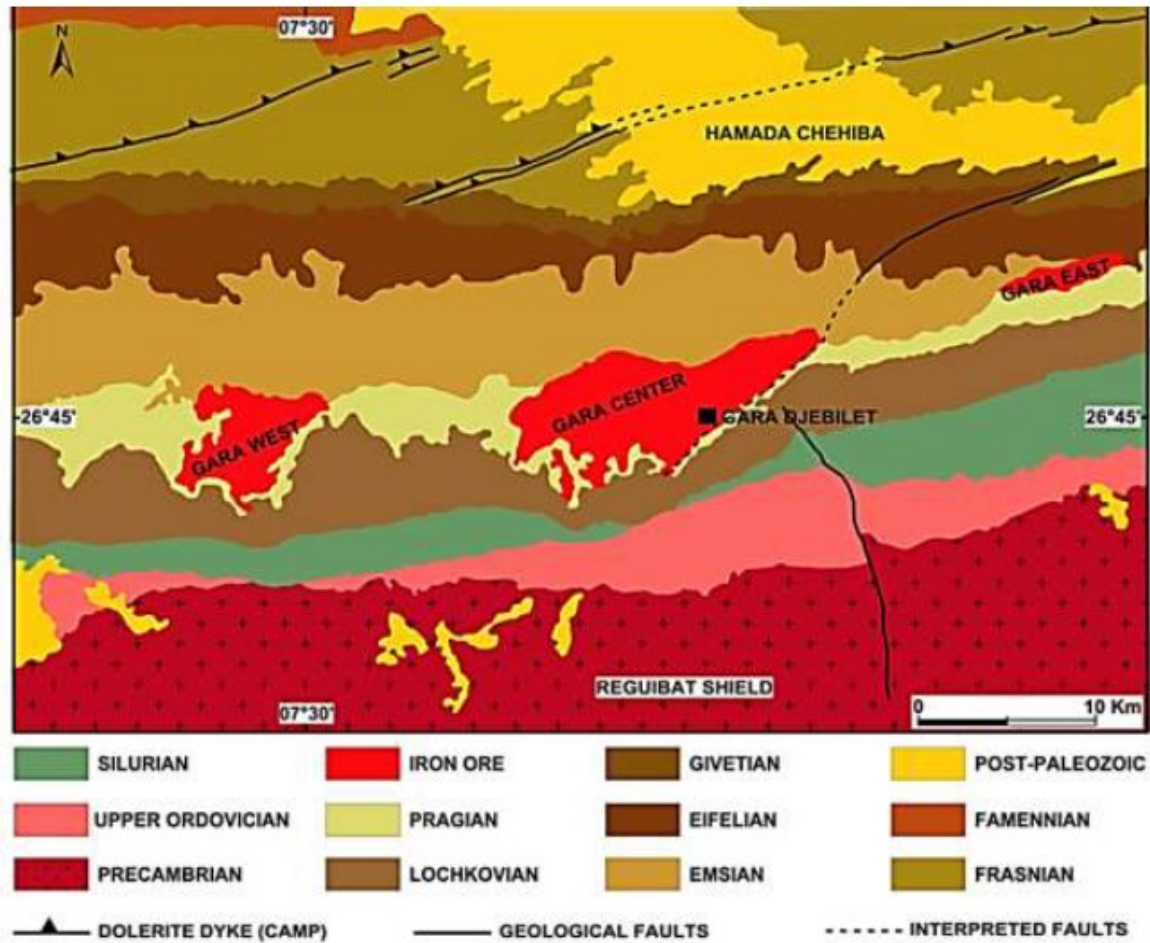


Fig 13: Geological map of the Gara-Djebilet region [28]

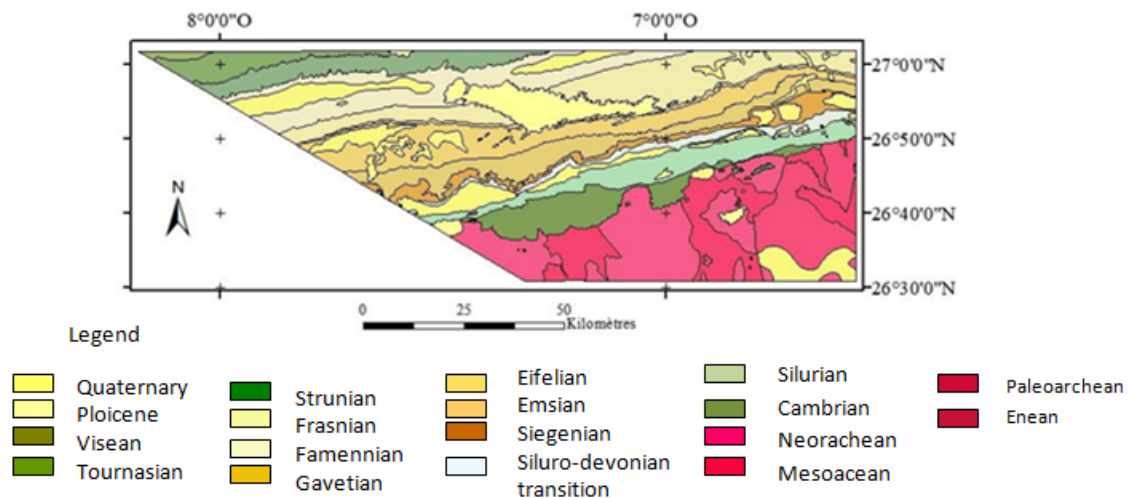


Fig 14: Geological map of the Gara-Djebilet [29]

The name of "formation of GaraDjebilet", consist mainly of sandstone with shales intercalations. It is divided into two members:

- ♣ The lower member "Sandstone of Djebilet" from the Lochkovian-Pragian age.
- ♣ The upper member "supra-mineral sandstone" from the Emsian age.

I-12-2Morphology and sedimentological

The deposit consists of three large lenses of oolitic iron ore, dipping slightly to the north (1.5° to 2°). These lenses are interstratified in clayey and sandy sediments; the sandstone host rock (classified as quartzarenite) is chloritic to ferruginous, containing more than 85% quartz and less than 15% matrix. The structure, and the synthetic lithostratigraphic column for each deposit are shown in Figure 10. It is clear that three coarsely ascending sequences (CUS), located between two sequences of ascending fineness (FUS) appear within the Gara Djebilet Formation: The first FUS concerns the Silurian marine transgression, consisting mainly of green and purple shales containing microfauna, such as graptolites; the first CUS corresponds to a sequence of progradation towards the sea, during which an incomplete foreshore covers an offshore plateau. [30]

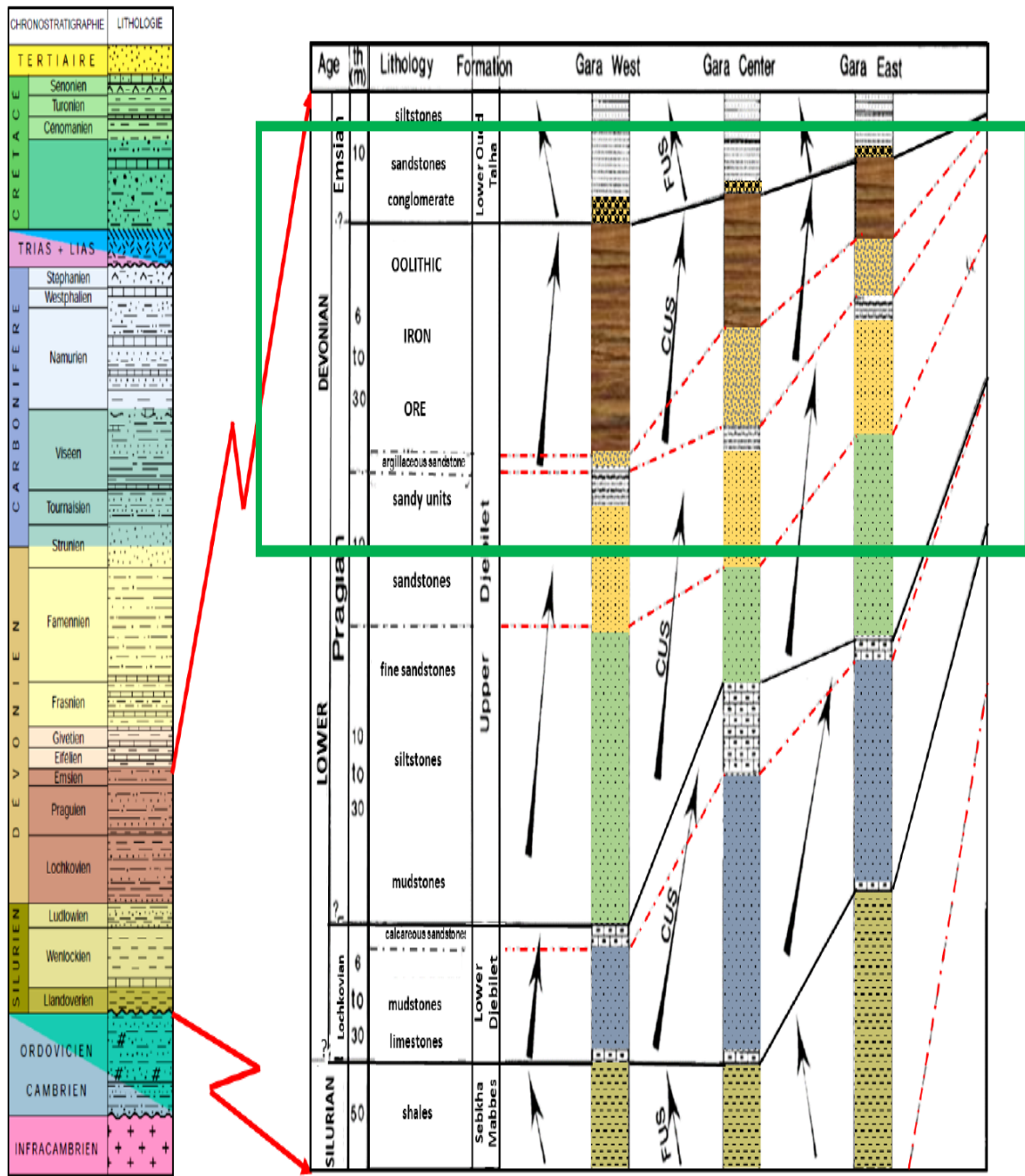


Fig 15: Lithostratigraphic columns of the Gara Djebilet deposit. [30]

The geodynamic evolution of the region took place in four stages: the Pan-African orogeny, the Caradocian tectonic compression, the Caledonian compression and the major Hercynian movements. All these tectonic movements took place during the Neoproterozoic to Permian period, and the majority of the lands of the Tindouf Basin were deposited in this time interval.

In the Gara Djebilet, a base and a cover have been distinguished. The base is made up of magmatic rocks while the cover, of a diversity of sedimentary rocks with limestones, sandstones and clays in majority. [29]

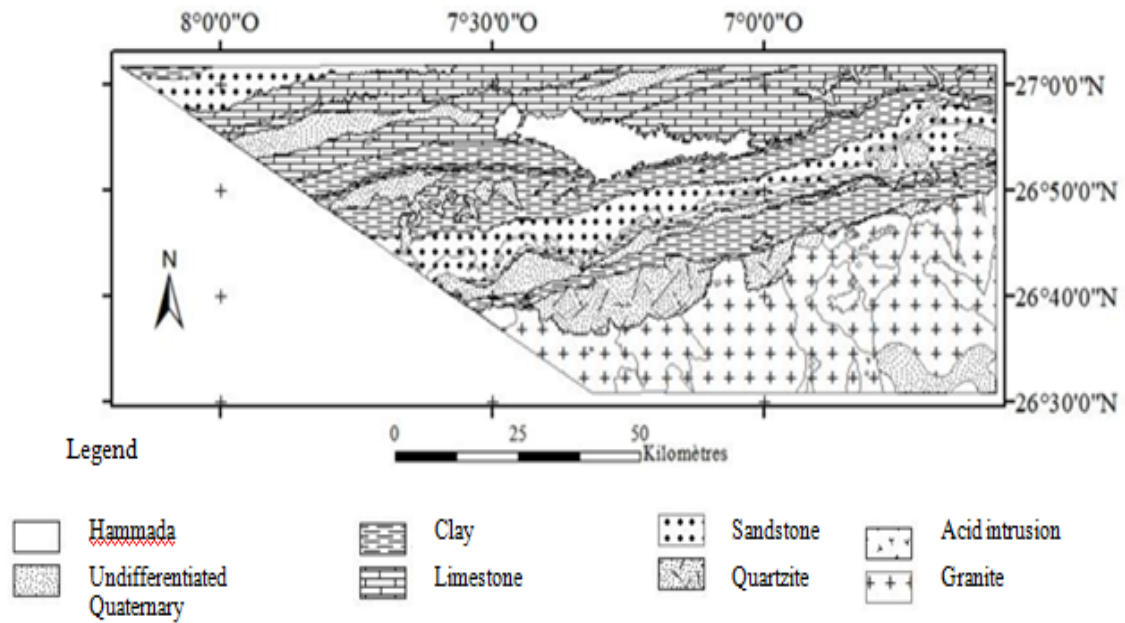


Fig 17: Map of Gara Djebilet facies [29]

I-12 Conclusion

The Gara Djebilet deposit is located approximately 140 km south-east of Tindouf, in south-west Algeria, close to the border with Western Sahara. From a geological point of view, Gara Djebilet is known as a major iron ore deposit. Geologically, it is located in the Hoggar region, part of the Saharan Atlas Mountains. The rock formations of the Gara Djebilet deposit consist mainly of sedimentary rocks, such as sandstone, limestone and shale, which host the iron minerals.

The geography allows concluding that the Gara Djebilet region is characterised by its desert environment. It is located in an arid zone of the Sahara, with very hot climatic conditions and little rainfall. Vast stretches of sand dunes and rocky plateaux are part of the region's characteristic landscape.

Structurally, the Gara Djebilet deposit is located in an area with a complex structure resulting from past tectonic activity. The region has been subjected to tectonic movements, such as folding, faulting and fracturing, which have influenced the formation of the iron ore deposit.

It is important to note that detailed geological studies are generally carried out to better understand the geology, geography and structure of the Gara Djebilet deposit. These studies help to determine the distribution of iron minerals, the configuration of the deposit and the most appropriate mining methods.

CHAPTER

11

II- Introduction

This passage discusses the importance of quantitative classifications of fractured rock massifs in feasibility and preliminary design studies of projects when information about the rock mass properties is not available. These classifications consider factors such as the strength of the rock matrix, water presence, and description of discontinuities. The goals of these classifications include estimating mechanical properties of the rock mass, determining stand up time, providing recommendations for support, and defining the stability of natural slopes or excavated slopes. The popularity of quantitative classifications lies in their ability to provide a common language between geologists, engineers, designers, and contractors and to better correlate observations, experience, and judgment of the engineers through the use of numbers instead of descriptions. [31;32;33;34;35;36]

II-1-Rock Quality Designation (RQD):

Deere (1964) proposes a parameter evaluating the rock quality of the rock mass according to an index called RQD (Rock Quality Designation). Obtained from geological drilling core, this index represents the evaluation of the percentage of core recovered over a length of recovered over a specified run length. Based on a qualitative process, only the sum of the lengths of pieces longer than 10 Cm is kept and this sum is divided by the run length of the core.[37;38]

$$RQD(\%) = \frac{\sum \text{piece lengths of more than 100 mm}}{\text{total length of core}} \times 100 \quad \text{II-1}$$



Fig 17: An example of RQD classification



Fig 18: Photos of drill core SA-007

Table II-1: The RQD index and the quality of the rock mass.

RQD (%)	Quality of the rock mass
<25	Very poor
25 - 50	Poor
50 - 75	Average
75 - 90	Good
90 - 100	Excellent

Table II-2: Value of the RQD

Layers	RQD (%)	Rock quality
High plasticity clay	61	average
Breccia	48	Poor
Layered clay	68.33	average
Sandstone (Coarse grained, medium grained and fine grained)	54.08	average
Ferruginous sandstone	66.87	average
Sandstone clay	78	Good
Argillite (mudstone/claystone, siltstone, shale)	81.5	Good
Ironstone	98	Excellent
Conglomerate(Ferruginous and carbonated)	<20	Very poor

The interpretation of the results:

RQD % total has benne 69,47 % Quality of the overall rock mass Average

II-2 Rock Mass Rating (RMR):

This classification was developed by Bieniawski [1973] at the South African Council of Scientific and Industrial Reasearch (SACSIR). It is based on the study of of a few hundred tunnels excavated mainly in sedimentary rocks at moderate depths. sedimentary rocks at moderate depths. The use of this classification requires the site into homogeneous regions from a geological structure point of view. geological structures. Each region is classified separately. The DPR is the sum of of five characterisation scores (A1 to A5) and one adjustment score.

The sum of these scores gives the massif a value between 0 and 100.

This value uses fracturing for more than 70% and gives 15% influence to the rock matrix properties and 15% to the properties of the rock matrix and 15% to the presence of water. [39; 40; 41]

The significance of the RMR indices is defined as follows:

- A1 (Strength of intact rock material);**
- A2 (Rock Quality Designation RQD);**

- A3 (Spacing of discontinuities);
- A4 (Conditions of discontinuities);
- A5 (Groundwater conditions).

$$\text{RMR}_{\text{basic}} = \text{A1} + \text{A2} + \text{A3} + \text{A4} + \text{A5}$$

II-2

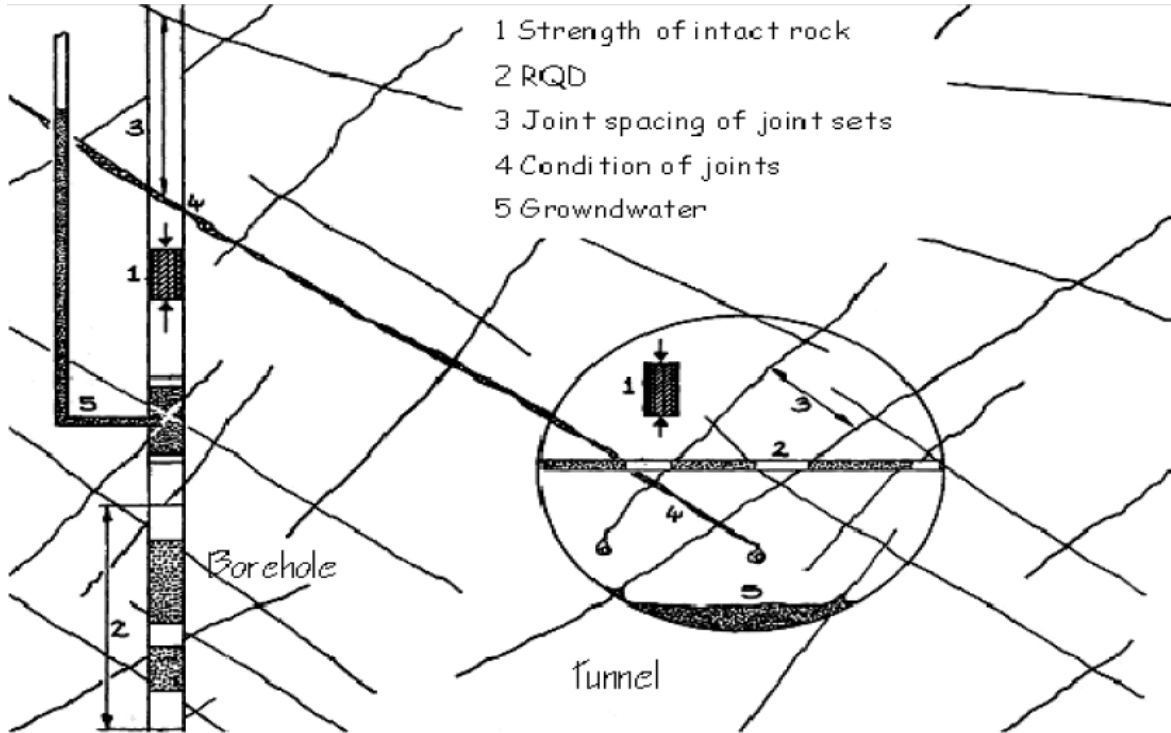


Fig 19: RMR characterisation parameters [52]

Table II-3 : RMR classification (Bieniawski, 1989)

PARAMETERS			COEFFICIENTS						
1	Rock strength (MPa)	Franklin index (MPa)	>10	4-10	2-4	1-2	Franklin index not usable (MPa)		
		Compressive strength (MPa)	>250	100-250	50-100	25-50	5-25	1-5	<1
		Note	15	12	7	4	2	1	0
2	RQD		100-90	90-75	75-50	50-25	<25		
	Note		20	17	13	8	3		
3	Joint spacing		>2m	0.6-2	0.2-0.6	0.06-0.2	<0.06		
	Note		20	15	10	8	5		
4	Nature of joints		Very rough non-continuous surfaces Contact sponge Unaltered sponge	Slightly rough surfaces Thickness <1 mm Sponge unweathered	Slightly rough surfaces Thickness <1 mm Altered sponge Surfaces	glossy or filling <5 mm or open joint 1 to 5 mm continuous joints	Filling >5 mm or open joints >5 mm continuous joints		
	Note		30	25	20	10	10		
5	Water ingress	Flow over 10 m	No water coming in	<10 l/min	10-25 l/min	25-125 l/min	>125 l/min		
		Water pressure main constraint	0	<0.1	0.1-0.2	0.2-0.5	>0.5		
		Hydrogeology	Completely dry	Moist	Seepage (interstitial water)	Moderate water pressure	Serious water problems		
		Note		15	10	7	4	0	

Table II-4: Classification of rock mass according to RMR (adapted from Bieniawski).

Massif class	RMR	Qualification
I	81 – 100	Excellent
II	61 – 80	Good
III	41 - 60	Average
IV	21 - 40	Poor
V	<20	Very weak

Table II-5: Value of the RMR

Facies		Ironstone				
Parameters	Rc(MPa)	RQD	Spacing of discontinuities	Conditions of discontinuities	Groundwater conditions	RMR
Measurement	87.11	98	0.6-2 m	Surfaces very rough not continuous Sponge in contact not altered	Completely Dry	87 I Excellent
Values extreme the classification						
Score	07	20				
Facies		Sandstone (Coarse grained, medium grained and fine grained)				
Parameters	Rc(MPa)	RQD	Spacing of discontinuities	Conditions of discontinuities	Groundwater conditions	RMR
Measurement	27.7	66.87	0.6-2 m	Surfaces very rough not continuous Sponge in contact not altered	Completely Dry	77 II Good
Values extreme the classification						
Score	4	13				
Facies		Argillite (mudstone/claystone, siltstone, shale);				
Parameters	Rc(MPa)	RQD	Spacing of discontinuities	Conditions of discontinuities	Groundwater conditions	RMR
Measurement	45	81.5	0.2-0,6 m	Surfaces slightly rough Thickness <1 mm Sponge Weathered	Completely Dry	66 II Good
Values extreme the classification						
Score	4	17				
Facies		Sandstone clayey				
Parameters	Rc(MPa)	RQD	Spacing of discontinuities	Conditions of discontinuities	Groundwater conditions	RMR
Measurement	43.2	68	0,6-2 m	Surfaces very rough not continuous Sponge in contact not Weathered	Completely Dry	72 II Good
Values extreme the classification						
Score	4	13				
Facies		Ferruginous sandstone				
Parameters	Rc(MPa)	RQD	Spacing of discontinuities	Conditions of discontinuities	Groundwater conditions	RMR

Measurement	55.9	66.87		Surfaces slightly rough		
Values extreme the classification			0,6-2 m	Thickness <1 mm	Completely Dry	75 II Good
Score	7	13	15	Sponge Not Weathered	15	

The interpretation of the results:

RMR total has benne 75.4 % Quality of the overall rock mass Good.

II-2-1 Estimation of the mechanical characteristics of rock masses using the RMR

The RMR can also be used to estimate the mechanical parameters of rock formations, such as such as cohesion and angle of friction. By estimating the average support time of an excavation of an excavation before support is applied. Several authors have proposed between these parameters and the value of the RMR. (Bieniawski.1989)

There are correlations that make it possible to estimate cohesion, the angle of friction as well as

Young's modulus:

II-2-1-a- Cohesion

$$-C_{eq} \text{ (kPa)} = 5 \text{ RMR, (Bieniawski, 1979)}$$

We have

Table II-6: Value of the cohesion

Facies	C_{eq} (kPa) $C_{eq} = 5RMR$
Ironstone	435
Sandstone (Coarse grained, medium grained and fine grained)	385
Argillite (mudstone/claystone, siltstone, shale);	330
Sandstone clay	360
Ferruginous sandstone	375

The interpretation of the results:

Ironstone: With a C_{eq} value of 435 kPa, ironstone is the strongest facies in terms of compressive strength. It is a dense and solid rock formation composed predominantly of iron minerals. Argillite (mudstone/claystone, siltstone, shale): The C_{eq} value of 330 kPa suggests a relatively weaker facies compared to ironstone and sandstone.

II-2-b- The angle of friction

$$\varphi_{eq}(\text{°}) = 0.5 \text{ RMR} + 8.3 \pm 7.2, \text{ (Trunck and Hönish, 1989)}$$

Table II-7: Value of the angle of friction

Facies	$\varphi_{eq}(\text{°})$ $\varphi_{eq} = 0.5RMR + 8.3 \pm 7.2$
Ironstone	36
Sandstone (Coarse grained, medium grained and fine grained)	39
Argillite (mudstone/claystone, siltstone, shale);	34
Sandstone clay	37
Ferruginous sandstone	39

The interpretation of the results:

The interpretation suggests a range of friction angles for different facies. Sandstone generally exhibits a higher friction angle compared to argillite, while ironstone tends to have a lower friction angle. These variations in frictional strength can have implications for slope stability, shear strength, and other geotechnical considerations.

II-3 Slope Mass Rating (SMR):

To evaluate the stability of rock slopes, Romana (1985) proposed a classification system called the "Slope Mass Rating" (SMR) system. SMR is obtained from Bieniawski (RMR) by subtracting the adjustment factors from the joint-slope relationship and adding a factor according to the excavation method.

$$\text{SMR} = \text{RMR}_{\text{basic}} + (F_1 + F_2 + F_3) * F_4 \quad \text{II-3}$$

F_1, F_2, F_3 are adjustment factors related to the orientation of the joints with respect to the orientation of the slopes, and F_4 is the adjustment factor related to the orientation of the slopes. The orientation of the joints in relation to the orientation of the slopes, and F_4 is the correction factor.

F_1 established empirically, it depends on the parallelism between the directions of the joints and the slopes. This factor can vary from 1 (when the two are almost parallel) to 0.15 (when the angle between the two is greater than 30° and the probability of failure is very low).

$$F_1 = (1 - \sin A)^2 \quad \text{II-4}$$

A is the angle between the directions of the joints and the slope.

F_2 depends on the dip of the joints for the planar failure mode. The values vary from 1 (for joints dipping more than 45°) to 0.15 (for joints dipping less than 20° dip). In the case of toppling, the factor remains equal to 1. It has also been established empirically by the following equation:

$$F_2 = \tan \beta_j \quad \text{II-5}$$

β_j is the dip of the joints.

F_3 is linked to the relationship between the slope of the slope and the dip of the joints. For this parameter, it is also necessary to differentiate between a flat failure and a toppling failure.

F_4 relates to the adaptation of the excavation method. Excavated cutting by pre-cutting, smooth shot blasting, normal shot blasting, poor blasting and mechanical excavation.

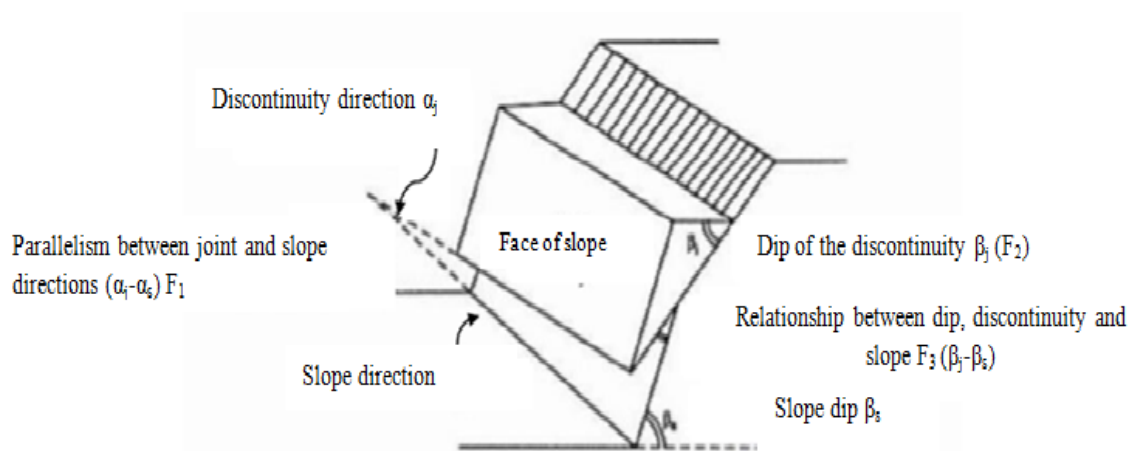


Fig 20: Orientation of a flat slope. [42; 43; 44;51]

Table II-8: Romana classification. [45; 46]

SMR = RMR _B +(F ₁ .F ₂ .F ₃)+F ₄					
Adjusting Factors for joint (F ₁ .F ₂ .F ₃)	α_j = Dip direction of joint α_s = Dip direction of slope		β_j =Dip of joint β_s =Dip of slope		
	very favourable	favourable	average	unfavourable	very unfavourable
Planar slip Toppling $\alpha_j - \alpha_s - 180$ = F ₁ value relationship	>30°	30°-20°	20°-10°	10°-5°	<5°
	0,15	0,40	0,70	0,85	1,00
	$F_1 = (1 - \sin \alpha_j - \alpha_s)^2$				
F ₂ value / plane failure /toppling relationship	$ \beta_j $ = <20°	20°-30°	30°-35°	35°-45°	>45°
	0,15	0,40	0,70	0,85	1,00
	$F_2 = \frac{1,00}{\text{tg}^2 \beta_j}$				
Plane failure Toppling F ₃ value Relationship	$\beta_j - \beta_s$ >10° $\beta_j + \beta_s$ <110°	10°-0° 110°-120°	0° >120°	0°-(-10°) --	<(-10°) ----
	0	-6	-25	-50	-60
	F_3 (Bieniawski adjustment ratings for joint orientation 1976)				
F ₄ Adjusting factor for excavation method	F_4 = Empirical values for method of excavation				
	Nature slope	presplitting	Smooth blasting	Blasting or mechanical	Deficient blasting
	+15	+10	+8	0	-8

Table II-9: The different stability classes by SMR value. [47; 48; 49; 50]

Classe	V	IV	III	II	I
SMR	0-20	21-40	41-60	61-80	81-100
Description	Very Poor	Poor	Normal	Good	Very Good
Stability	Completely unstable	Unstable	Partially stable	Stable	Completely stable
fall	Large plane, ground or circular	plan	Large plan	fall of bocs	No fall
Probability of fall	0.9	0.6	0.4	0.2	0

Knowing that the directions of the slope of the cliff going of direction 170° and 80° dip which are measured in the site i.e:

$$\alpha_s = 170^\circ$$

$$\beta_s = 80^\circ$$

And the mean vector is:

Direction α_j 120° its plunge β_j 7°

Table II-10: SMR values

Parameters	Value	SMR value
RMR_{Basic}	87	75.4
F_1	0.4	
F_2	0.15	
F_3	-60	
F_4	-8	

Interpretation of the results

We can see that the value of the SMR in class II indicates that the slope is of good quality and stable. Conclude that the slope is of good quality and stable, with no flat or dihedral falls with a probability of fall equal to 0.2 (see Table II-9).

II-4 Conclusion

Based on the information provided, you have presented several semi-empirical classification methods for rock masses. You have also highlighted a number of key points. Empirical classification systems such as RQD (Rock Quality Designation), RMR (Rock Mass Rating) and SMR (Stress Measurement Ratio) are considered simple.

The geomechanical characterisation of rock masses essentially consists of quantifying the structural elements of the rock mass. These classifications, which are both descriptive and quantitative, are used to assess the quality of the rock mass.

In the case of the specific iron rock mass you mention, it is composed of alternating clayey sandstones and clays at the base, over which conglomerate and quaternary deposits have formed. Classified as a good rock

CHAPTER

III

III- Introduction

The geotechnical study plays an essential role in the new opening of a mine. The main objective of this study is to assess the geological, geotechnical and hydrogeological characteristics of the mine site in order to determine the soil and rock conditions, as well as the constraints to which the mine will be subjected.

The geotechnical study for a new mine opening generally takes several aspects into account:

Bedrock assessment: An in-depth study is carried out to understand the geological composition of the soil and underlying rock. This often involves geophysical investigations, coring and sampling to determine the physical and mechanical properties of the geological formations.

Slope stability: The geotechnical study assesses the stability of the slopes in the area of the future mine. This includes an analysis of the risk of landslides, rockfalls or other ground movements that could compromise the safety of mining operations.

Soil characteristics: The geotechnical study provides an understanding of soil characteristics such as bearing capacity, permeability, compressibility and other mechanical properties. This information is crucial for the design of mining infrastructure, including excavations, access roads, work platforms, etc.

Groundwater management: The geotechnical investigation also assesses hydrogeological aspects, including water table levels, groundwater flow and measures required to manage groundwater during mining operations.

The geotechnical study in the context of opening a new mine provides essential information for designing and planning mining operations while minimising geotechnical risks. It helps to ensure the safety of workers, the sustainability of infrastructure and the long-term profitability of mining operations.

III-1 Laboratory test

The samples taken were subjected to physico-mechanical tests. The LCTP and ITU carried out laboratory tests in accordance with FERAAL's request. Following:

- Granulometric analysis: (NF P94-056);
- The Atterberg limits: (NF P94-051);
- Shear tests at the Casagrande box: (NF P94-071-1);

- Determination of Physical properties (density): (NF P94-053);
- Compressive strength (UCS): (NF EN 12 504-1);
- Triaxial shear tests (NF P94-074).

III-2 Results of the tests carried out

III-2-1 Granulometric analysis (NF P94-056)

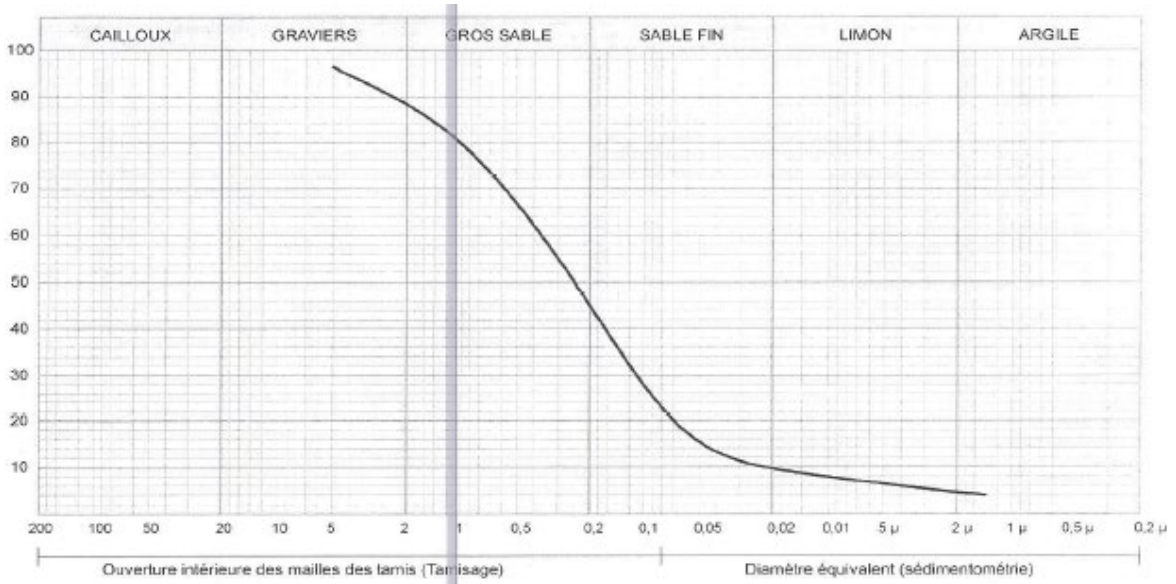


Fig 21: Particle size curve ZK08/0.2-0.7 (Fine-grained sandstone)

III-2-2 The Atterberg limits: (NF P94-051)

Table III-1: Value of the Atterberg limits

Sounding	Depth (m)	LI (%)	Lp (%)	Ip (%)	Soil qualification
ZK 08	0.20 – 0.70	20.04	12.56	7.48	Non-plastic clay (CL)

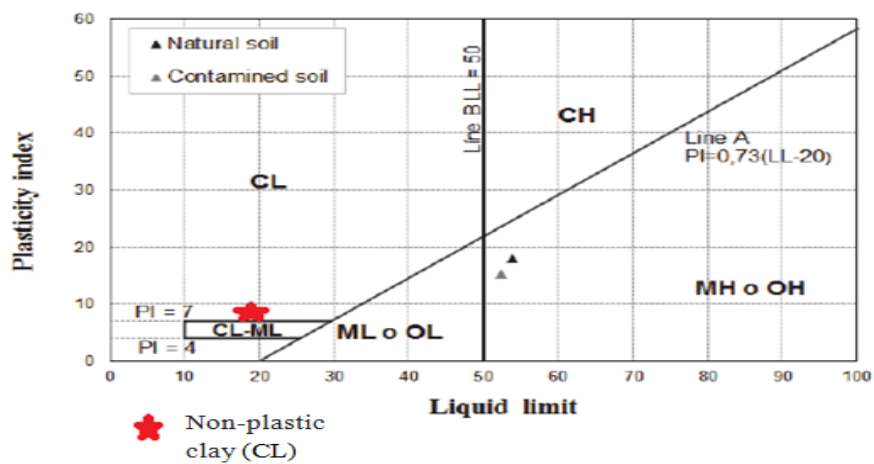


Fig 22: Curve of Atterberg limits ZK08/0.2-0.7

III-2-3 Shear tests at the Casagrande box (NF P94-071-1) He drained consolidated direct rectilinear shear test (CD), gave the following results

Table III-2: Value of the cohesion and Angle of internal friction in degrees

Sounding	Depth (m)	Type of test	C'(Kpa)	ϕ°
ZK03	46.77-47.05	CD	82.25	10.50
ZK10	37.50-37.75		97.68	09.00

III-2-4 Determination of Physical properties (density) (NF P94-053)

Table III-3: Physical properties test results

Sample No	Depth (m)	Natural Weight (g)	Dry Weight (g)	Saturated Weight (g)	Water content (%)	Dry density (g/cm ³)	Water Absorption %	Porosity %	Lithology
ZK-3	14.40 - 14.60	646.05	633.76	691.63	1.9	2.31	9.1	21.1	CS
ZK-5	21.20 - 21.85	811.59	803.63	882.11	1.0	2.78	9.8	27.1	FOC
ZK-7	45.75 - 45.97	863.44	855.69	895.00	0.9	2.83	4.6	13.0	CS
ZK-7	36.32 - 36.59	915.63	907.46	932.82	0.9	3.19	2.8	8.9	SS
ZK-3	30.16 - 30.40	825.00	821.23	847.66	0.5	2.55	3.2	8.2	CS
ZK-4	20.37 - 20.62	724.64	722.57	738.56	0.3	2.47	2.2	5.5	SS
ZK-5	24.22 - 24.56	776.30	769.95	827.46	0.8	2.94	7.5	21.9	FOC
ZK-10	23.15 - 23.65	928.20	904.73	979.90	2.6	2.53	8.3	21.0	SS

The interpretation assumes that the values represent the dry density, water absorption, porosity, and lithology of the samples respectively. The lithology abbreviations correspond to specific rock types.

III-2-5 Compressive strength (UCS) (NF EN 12 504-1)

The results of the uniaxial compressive strength tests in the natural state (RC) are shown in the following table

Table III-4: Value of the uniaxial compressive strength

Sounding	Depth (m)	Ø (cm)	H (cm)	H/D	LOAD (kN)	Compressive strength (ucu)(Mpa)
ZK2	16,5-16,87	9,26	20,3	2,13	124,6	18,5
ZK3	35-35,33	9,33	20,56	2,15	296,6	43,4
Zk5	24,22-24,56	9,39	20,34	2,09	387,8	55,9
ZK5	32.07-32.28	9.39	20.5	2.18	325,2	47.0

Table III-5: Value of the young's module and poison ration

Sounding	Depth (m)	Rock description	Young's Module (GPa)	Poison ration
ZK2	16,5-16,87	SS	5,262	0,16
ZK3	35-35,33	CS	11,007	0,16
Zk5	24,22-24,56	FOC	18,477	0,17
ZK5	32.07-32.28	CS	10,516	0,31

Interpretation table IV-4 and table IV-5: FOC has the highest Young's modulus of the rocks mentioned, indicating high rigidity. Its Poisson's ratio is slightly higher than that of the other rocks, suggesting relatively greater deformability. FOC has the highest compressive strength, which means it is more resistant to compressive loads. These rocks have different mechanical properties, particularly in terms of stiffness, deformability and compressive strength. These characteristics are important for understanding how rocks react to the forces and stresses applied to them.

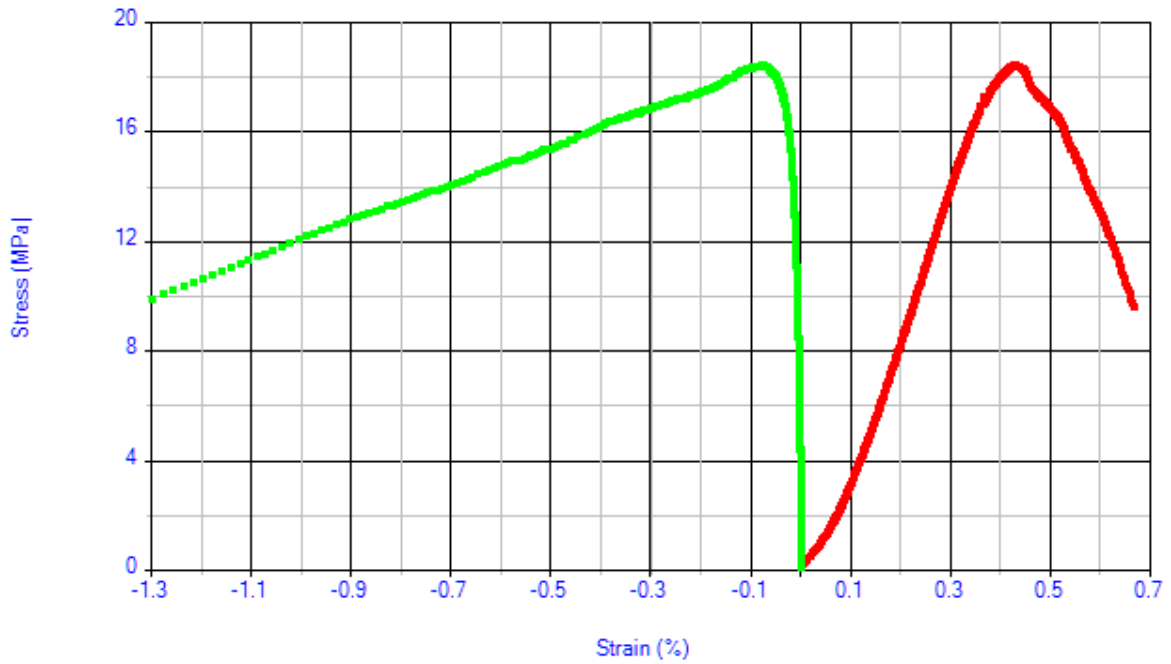


Fig 23: Stress – strain graph for ZK02

The given information states that the maximum stress (compressive strength) for a particular rock is 18.5 MPa. This stress is reached at a corresponding strain (deformation) of 0.43%. Beyond this point, the rock experiences rupture or failure.

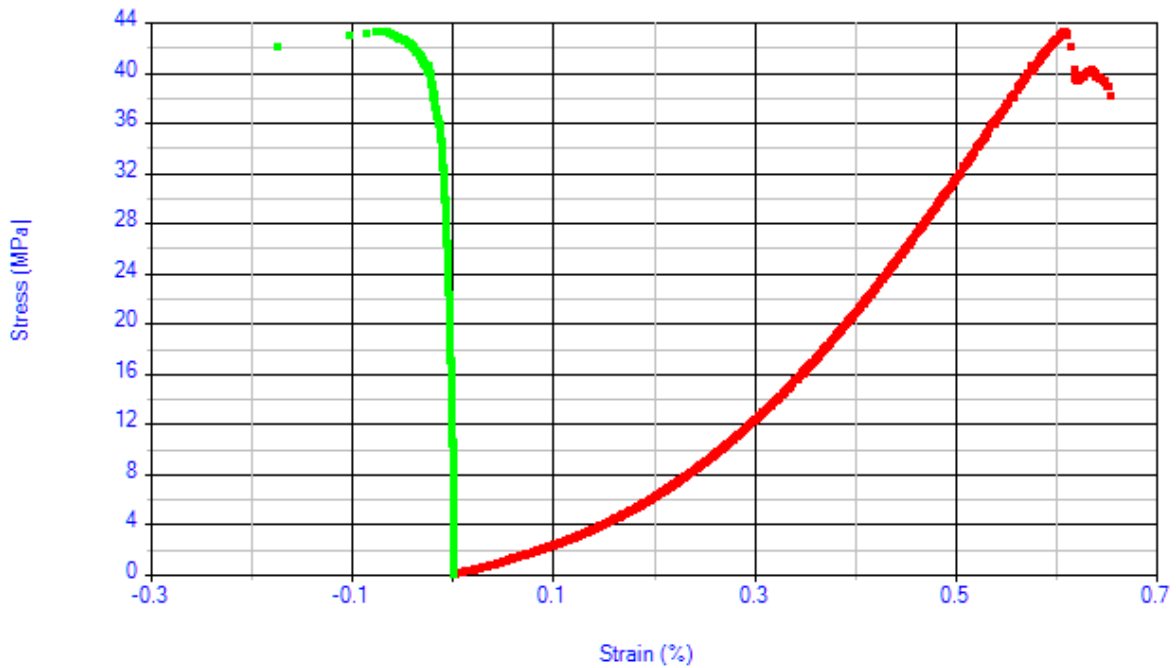


Fig 24: Stress – strain graph for ZK03

The given rock has a maximum stress (compressive strength) of 43 MPa. This stress is reached when the rock undergoes a strain (deformation) of 0.6%. If the strain exceeds this value, the rock will experience rupture or failure.

III-2-6 Direct Shear Tests

Table III-6: Direct shear test results for DSTJ & DSTW.

Sample	Depth	Lithology	Test Results				Shear strength properties	
			Normal Force (KN)	Normal Stress (MPa)	Max shear Strength	Residual Shear strength	Max cohesion MPa	Max friction angle °
ZK3	37,5-37,81	CS	2	0,29	0,44	0,29	0,23	33,82
			4	0,65	0,65	0,57		
			6	0,97	0,89	0,73		
ZK8	7,66-7,84	SS	2	0,29	0,43	0,29	0,26	36,87
			4	0,58	0,79	0,58		
			6	0,87	0,87	0,65		

Interpretation: For both lithologies, the test results indicate the applied normal forces and the resulting normal stresses. The shear strength properties describe the maximum shear strength, residual shear strength, maximum cohesion, and maximum friction angle, the CS chalkstone exhibits a higher maximum cohesion of 0.23 MPa compared to the sandstone (SS) with a maximum cohesion of 0.26 MPa. However, the sandstone has a slightly higher maximum friction angle of 36.87° compared to the chalkstone with a maximum friction angle of 33.82°. These values provide insights into the shear strength characteristics of the respective lithologies and are important for understanding their stability and behavior under shear forces.

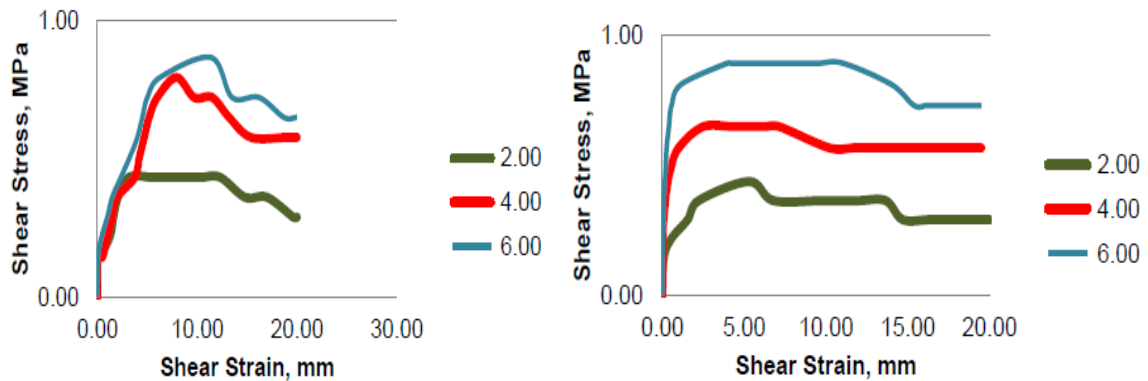


Fig 25: Shear stress-strain graph for ZK-8 and ZK-3

Interpretation: The graphs show the relationship between shear stress τ and strain ϵ for different values of Sigma 3. The specific values of displacement are also given for each value of Sigma 3, which makes it easier to understand the relationship.

For Sigma 3 = 2 MPa :

- The shear rate is 0.45 MPa for a displacement of 4 mm.

For Sigma 3 = 4 MPa :

- The shear rate is 0.73 MPa for a displacement of 8.38 mm.

For Sigma 3 = 6 MPa :

- The shear rate is 0.87 MPa for a displacement of 13 mm.(for ZK-8)

For Sigma 3 = 2 MPa :

- The shear rate is 0.35 MPa for a displacement of 5 mm.

For Sigma 3 = 4 MPa :

- The shear rate is 0.65 MPa for a displacement of 3 mm.

For Sigma 3 = 6 MPa :

- The shear rate is 0.9 MPa for a displacement of 4.7 mm (for ZK-3)

From these data, an increase in shear stress can be seen as strain increases for each value of Sigma 3. This indicates a direct relationship between shear stress and strain, where an increase in strain leads to an increase in shear stress.

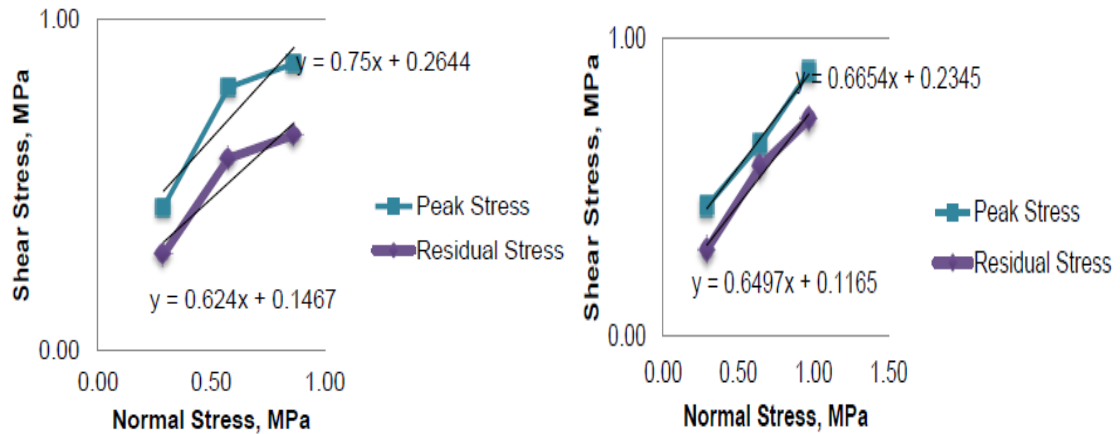


Fig 26: Shear and normal stress graph for ZK-8 and ZK-3

Interpretation: Indeed, from the formulas provided, it seems that peak stress is generally higher than residual stress. This can be interpreted as follows:

Peak stress represents the maximum value of shear stress reached when normal stress is at its highest. The corresponding shear stress will increase more rapidly with increasing normal stress.

The residual stress, on the other hand, is the shear stress that remains after the normal stress has been removed. The residual shear stress is generally lower than the peak shear stress, with a smaller slope and a lower constant.

These results suggest that the shear stress is higher when there is an applied normal stress, but decreases when the normal stress is removed.



Fig 27: Uniaxial Compressive Strength Sample ZK03
A (Before) B (After)

III-3 In addition to what we brought from the Feraal, in the geotechnical laboratory of the University of ChahidCheikhLarbiTabssi, we carried out ultrasonic tests and specific gravity load test we obtained results summarized in tables

III-3-1 Density of ironstone:



Fig 28: Photo of realization the density of ironstone

Table III-7: Value density of ironstone

N° sample	Density (g/cm ³)
N° 1	3,37
N° 2	3,69
N° 3	3,78
N° 4	3,78
N° 5	3,71
N° 6	3,71
N° 7	3,79
N° 8	2,95
N° 9	3,44
N° 10	3,33
N° 11	3,23
Mean	3,53

Interpretation of the results shows the densities of the different iron samples (ironstone). Here is an interpretation of the results:

The densities of the ironstone samples vary in the following range:

- The minimum density is 2.95 g/cm³.
- The maximum density is 3.79 g/cm³.

This suggests that ironstone samples show a variation in density, with some samples having a lower density and others a higher density. It is also important to note that density is a physical property that can be influenced by various factors, such as the chemical composition, crystal structure and porosity of the ironstone sample.

III-3-2 Ultrasonic tests

Ultrasonic tests are commonly performed on soil and rock samples to determine their physical and mechanical characteristics. In reality, ultrasonic tests do not directly determine Young's modulus and Poisson's ratio. But by formulas of the values of Vp and Vs (which obtained by ultrasonic test) and also density .



Fig 38: Photos of realization ultrasonic test of ironstone

$$\nu = \frac{1 - 2\left(\frac{V_L}{V_T}\right)^2}{2 - 2\left(\frac{V_T}{V_L}\right)^2} \quad \text{III-1}$$

$$E = \rho V_L^2 \frac{(1-\nu)(1-2\nu)}{(1-\nu)} \quad \text{III-2}$$

V_L : Longitudinal speed (m/s)

V_T : Transverse Speed (m/s)

E: young's modulus (GPa)

ν : poison coefficient

ρ : density (kg/m³)

Table III-8: Value poison coefficient and young's modulus of ironstone

poison coefficient	Young's modulus (GPa)
0,27	135
0,20	152
0,33	44,1

Interpretation: These results indicate that ironstone samples have different deformation behaviours. Poisson's ratio values range from 0.20 to 0.33, suggesting different degrees of lateral contraction or expansion when subjected to stress. In addition, Young's modulus values range from 44.1 GPa to 152 GPa, reflecting different levels of stiffness and resistance to deformation.

III-3-3 Test FRANKLIN (PLT): Test is a simple and rapid method to estimate the strength of rocks and hard materials.

D: equivalent diameter in mm

F: maximum force in N

σ_c : The index of resistance to compression under point load.

$$PLT = F/D^2 \quad \text{IV-3}$$



Fig 30: Photos of realization test point load

Table III-9: Value de PLT and resistance of compression under point load

N°	D (m)	AIRE (m ²)	F (KN)	IS (KPA)	σ _c (KPA)
1	0,065	4,2.10 ⁻³	9,71	2311,90	55485,71
2	0,0657	4,48.10 ⁻³	16,6	3705,36	88928,57
3	0,0657	4,48.10 ⁻³	13,98	3120,54	74892,86
4	0,0657	4,554.10 ⁻³	7,11	1561,26	37470,36
5	0,0657	4,554.10 ⁻³	12,15	2667,98	64031,62
6	0,0657	4,554.10 ⁻³	16,53	3629,78	87114,62
7	0,0735	5,402.10 ⁻³	12,7	2350,98	56423,55
8	0,0735	5,402.10 ⁻³	14,74	2728,62	65486,86

Interpretation: The results of the Franklin tests on the ironstone samples showed a variation in normal stress values in the range 2311.90 kPa to 3629.78 kPa. These values correspond to the stress levels applied to the samples during the Franklin tests.

Compressive strength values range from 55485.71 kPa to 88928.57 kPa. These values indicate the ability of ironstone samples to withstand applied compressive forces before undergoing deformation or fracture.

III-4 Conclusion

A series of geotechnical laboratory tests have been conducted to analyse and obtain the different geotechnical parameter of

When conducting geotechnical laboratory tests to analyze and obtain geotechnical parameters for rock masses, several tests can be performed. These tests provide valuable information about the engineering properties and behavior of rock materials. Here are some commonly conducted geotechnical laboratory tests for rock masses and the parameters they help determine:

Uniaxial Compressive Strength (UCS) Test: This test is used to determine the maximum compressive strength of a rock sample. It involves applying axial load to a cylindrical or cubical rock specimen until failure occurs. The UCS value indicates the rock's ability to withstand compressive stresses.

Point Load Index Test (PLI): This test is an indirect measure of rock strength and is used when intact rock cores are not available. A load is applied to a rock specimen using a specialized point load apparatus, and the peak load is recorded. The PLI value can be used to estimate the uniaxial compressive strength and the rock mass rating (RMR).

These laboratory tests, along with in-situ testing and field observations, help characterize the geotechnical properties of rock masses. The obtained parameters are crucial for rock engineering projects, slope stability analysis, as they aid in understanding the behavior and response of rock masses under different loading and environmental conditions.

CHAPTER

IV

IV- introduction

Long-term slope stability in open-cast quarries is a major issue facing mines around the world. We will examine traditional methods of slope stability analysis, such as the limit equilibrium method, as well as more advanced approaches, such as numerical models and probabilistic methods. We will discuss the advantages and limitations of each method and propose an integrated approach to estimating the actual safety of embankments.

IV-1-Slope stability calculation

Ground stability calculation methods are based on the following observation:

When there is a landslide, there is separation of a mass of soil from the rest of the massif and its sliding takes place along a rupture surface. Having defined a failure surface “S”, the stability of the mobile mass (1) relative to the solid mass (2) which is fixed is studied. [53;54;55]

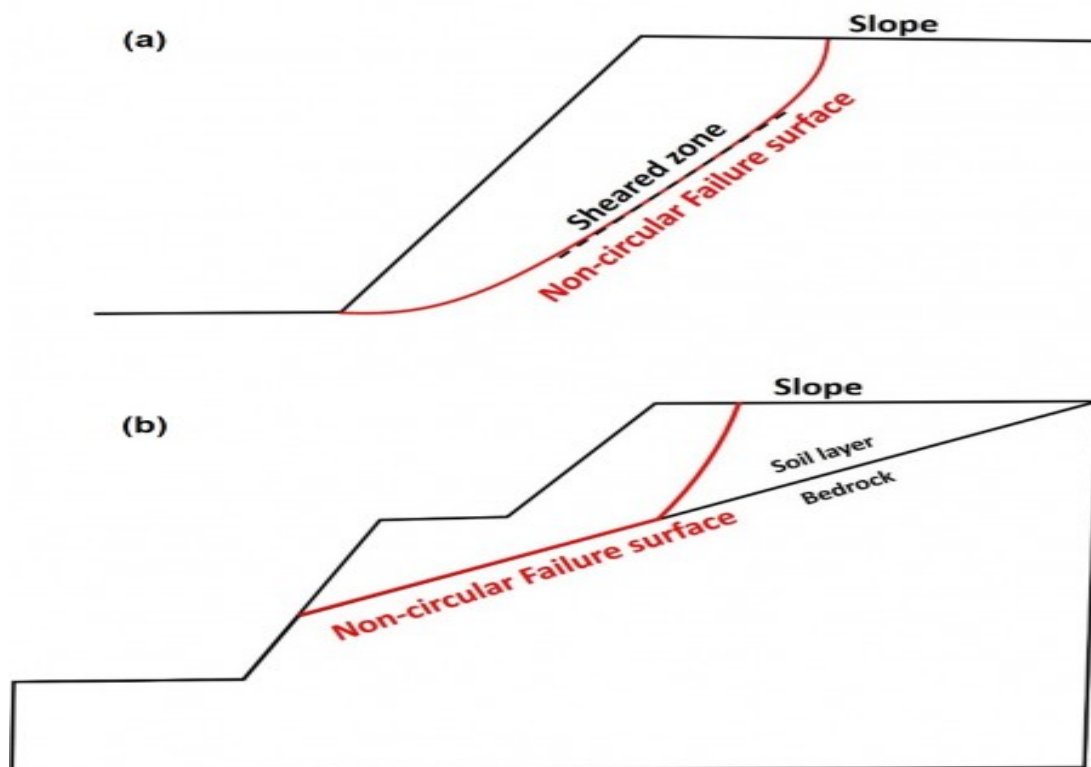


Fig 31: Description of the failure surface. [54]

IV-2- Definition of the safety factor

The slope stability calculation is generally estimated using a coefficient called:

Safety factor F_s . This coefficient is defined as being the ratio of moment to relative to a fixed point of the resultant of the forces resisting slipping to the forces causing slippage. [53; 55; 56; 57]

$$F_s = \frac{\text{moments of forces resisting motion}}{\text{moments of forces causing motion}} \quad \text{IV-1}$$

Theoretically: $F_s > 1$, the slope is stable.

$F_s < 1$, the embankment can only slip.

$F_s = 1$, the slope is in a state of limit equilibrium.

In practice, the state of stability may require values of F_s between 1.15 and 1.30

Up to 1.50 and those, taking into account the following factors:

- Errors due to the accuracy of edge stability calculation methods.
- The experimental uncertainties of the determination of the physico-mechanical properties of the rocks, such as the average value of the specific weight of the rocks composing the mass.
- The uncertainties of the determination of the influence of cracking.
- The influence of the dynamic loads caused by the shot, by the movement of the means transportation and seismic activity. [54 ; 58]

IV-3- Calculation methods

The main methods for calculating slope stability are:

- Methods based on limit equilibrium.
- Finite element methods.
- Abacus methods.

In the second part of our work, we will use finite element methods (FEM).

IV-4-Methods based on limit equilibrium (slice method)

The so-called limit equilibrium calculation methods are based on an assumption of a mechanism of rupture a priori according to sliding surfaces, and the analysis of the stability of the part of the massif delimited by these failure surfaces.

From a conceptual point of view, the main drawback of these methods is that they can lead to solutions that are higher than the actual limit loads on the structures (Coussy and Salençon, 1979).[59; 60]

This method consists in considering the forces which tend to retain a certain volume of terrain, bounded by free slope forces and a potential failure surface, and those that tend to set it in motion. Fig 24 and 25 Illustrate the principle of the slice method: [54]

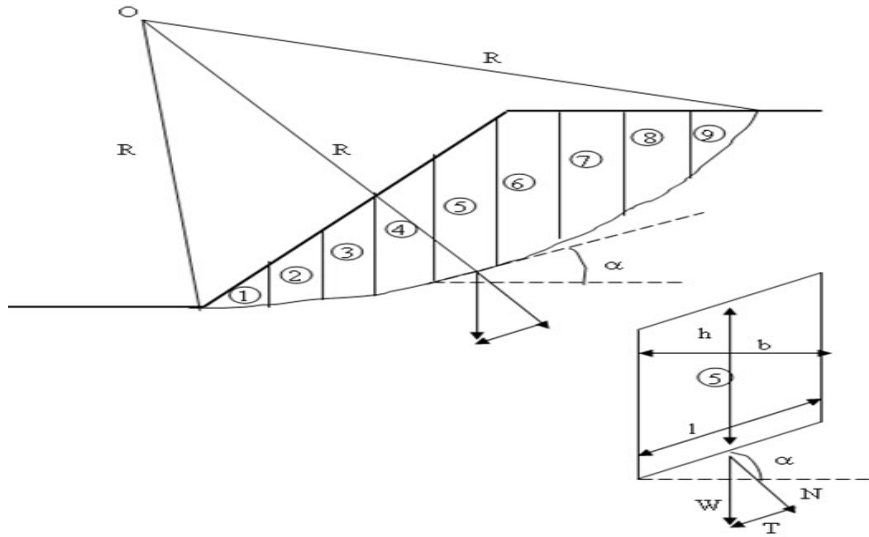


Fig 32: Description of slicing with breaking surface. [54]

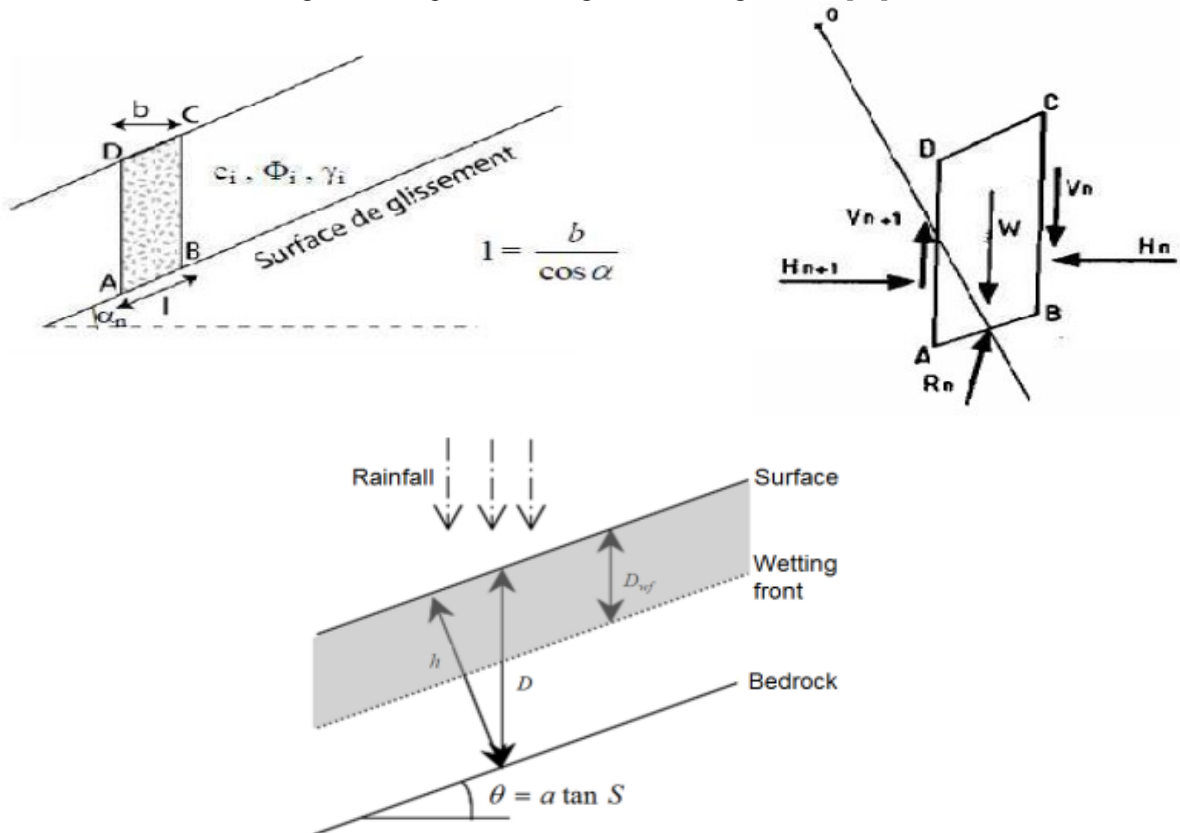


Fig 33: Demonstration of forces acting on a wafer. [54]

Let be any circle with center O and radius R for which we verify security with respect to the risk of slipping. The method of slices consists in cutting the volume of the ground (included in the arc EF) in a certain number of slices bounded by vertical planes.

In the absence of water, a section (n) is subjected to:

His weight $W = \gamma_n \cdot h_n \cdot b_n$

(in these cases one considers the problem in 2D, the thickness equal to the unit).

- The inter-slice forces broken down into horizontal forces H_n and H_{n+1} and in vertical forces V_n and V_{n+1}
- The reaction R_n of the underlying medium on the arc AB (shear resistance). It breaks down into a normal component and a tangential component.

IV-4-1- Method of FELLENIUS (1936)

Also called Swedish method or ordinary method, it is considered that:

- The slip line is circular.
- One totally neglects the forces inter-sections (horizontal and vertical).
- The only force acting on the arc AB is the weight W.

The equilibrium studied is the equilibrium of moments. [61; 62; 63]

With respect to the center O, we can define:

- The driving moment like that of the weight of the land W tending to cause slippage.
- The maximum resistant moment provided by the maximum value that the component can take tangential of R_n

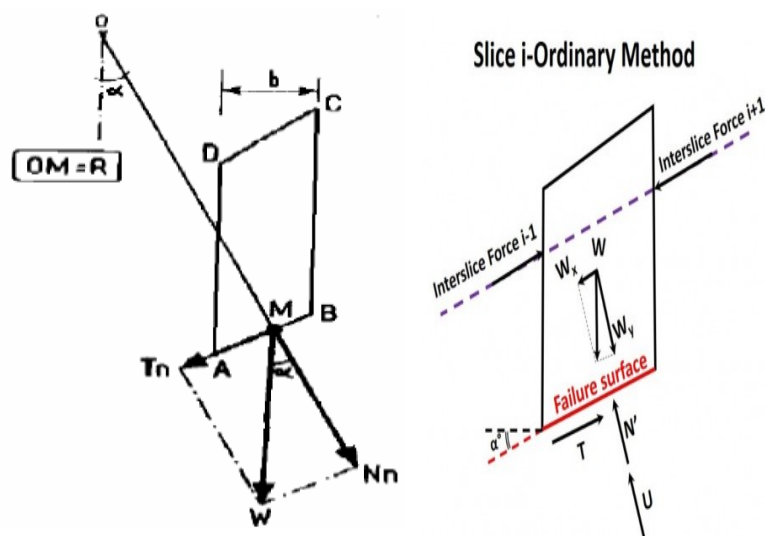


Fig 34: Forces acting on a surface according to FELLENIUS. [53]

According to Coulomb's law:

$$R_n = C_n * AB + N_n * \tan\varphi_n \quad \text{IV-2}$$

With:

$$N_n = W_n * \cos\alpha_n \quad \text{IV-3}$$

SO:

$$R_n = C_n * AB + W_n * \cos\alpha_n * \tan\varphi_n \quad \text{IV-4}$$

And we have:

$$AB = I_n = \frac{b_n}{\cos\alpha_n} \quad \text{IV-5}$$

The Sum of the maximum resistant moments is written:

$$= \sum_{n=1}^m (C_i * \frac{b_n}{\cos\alpha_n} + W_n * \cos\alpha_n * \tan\varphi_i) \quad \text{IV-6}$$

The sum of the maximum resistant moments is written:

Where: m: the number of slices.

C_i, φ_i : mechanical characteristics of the layer in which the arc AB is located.

-the driving moment is due to T_n is equal to $T_n * R$

Moreover:

$$T_n = W_n * \sin\alpha_n \quad \text{IV-7}$$

By substituting (III-6) and (III-7) in equation (III-1), we obtain the expression for the factor of security

$$F_s = \sum_{n=1}^m (C_i * \frac{b_n}{\cos\alpha_n} + W_n * \cos\alpha_n * \tan\varphi_n) \div \sum_{n=1}^m W_n * \sin\alpha_n \quad \text{IV-8}$$

The parameters involved in the calculation of F_s thereby are:

- b: the width of the slices.

- α : the oriented angle made by the radius of the circle passing through the middle of the base of the slice with the vertical.

-The height of the slice for the calculation of the weight W.

Fellenius' method gives pessimistic results compared to Bishop's method simplified.

Deviations on F_s can reach 10%. The Fellenius method has the advantage of simplicity and therefore can be used in all common cases.

IV-4-2- Simplified BISHOP method (1954)

In this method we consider that:

- The slip line is always circular.

- The equilibrium studied is the equilibrium of moments.
- The horizontal inter-slice forces are zero. [61; 64; 54]

The safety factor is given by the following formula:

$$F_s = \sum_{n=1}^m \left(\frac{C_i * b_i + W_i * \tan \varphi_i}{m_a \sum_{n=1}^m W_i * \sin \alpha_i} \right) \quad \text{IV-9}$$

With:

$$m_a = \cos \alpha_i \left(1 + \frac{\tan \alpha_i * \tan \varphi_i}{F_s} \right) \quad \text{IV-10}$$

To determine F_s it is necessary to proceed by successive iterations, the first iteration is made by adopting as value F_s the safety factor obtained by the Fellenius method.

It is therefore an indirect (or iterative) method and it only checks the balance of the moments, just like the Fellenius method (does not check the balance of forces). [53]

III-4-3- JANBU method (1956)

Janbu's method determines the factor of safety by the balance of forces. This method considers the normal forces between the slices (E), but neglects the forces of shear (T). The normal force (P) is determined as in Bishop's method simplified. [65; 66]

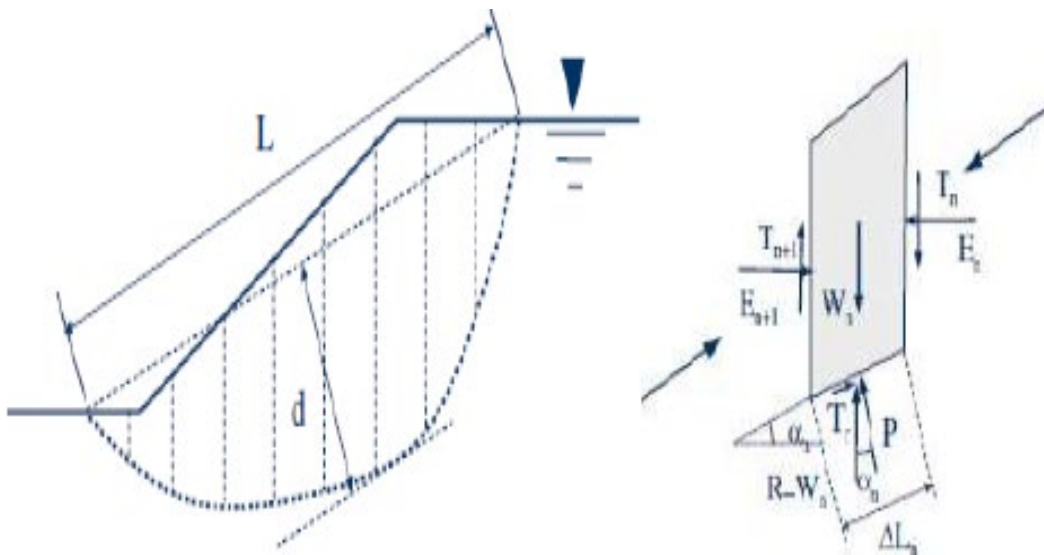


Fig 35: Forces considered in Janbu's method. [66]

Janbu first calculates an uncorrected safety factor F_{s0} which is determined as follows

$$F_{s0} = \frac{\sum_{n=1}^m (b_n \frac{\tan \phi_i [C_i + \frac{(W_n - v)}{b_n}]}{n_a})}{\sum_{n=1}^m W_n \tan \alpha_n} \quad \text{IV-11}$$

With:

$$n_a = \cos^2 \left(1 + \tan \alpha_n * \frac{\tan \phi_i}{F_{s0}} \right) \quad \text{IV-12}$$

(W_n/b_n) is the total vertical stress.

b_n is the width of slice n .

α_n : the inclination of the sliding surface in the middle of slice n .

u : pore water pressure.

One can notice that the method of Janbu, satisfies the balance of the forces and considers the inter-slice normal forces (E). It is an indirect method (iterative, since F_{s0} is two sides of the equation). It is generally used for a shear surface compound (general sliding surface).

Janbu introduced a correction factor (f_0), in the original safety factor, for compensate for the effects of inter-slice shear forces. With this modification, the method from Janbu gives higher values of the safety factor F_s , such as:

$$F_s = f_0 * F_{s0} \quad \text{IV-13}$$

The correction factor depends on the ratio between depth and length of the surface of rupture (d/L). The safety factor with this correction factor can increase from 5 to 12%, giving a lower margin in the case of friction alone. [61]

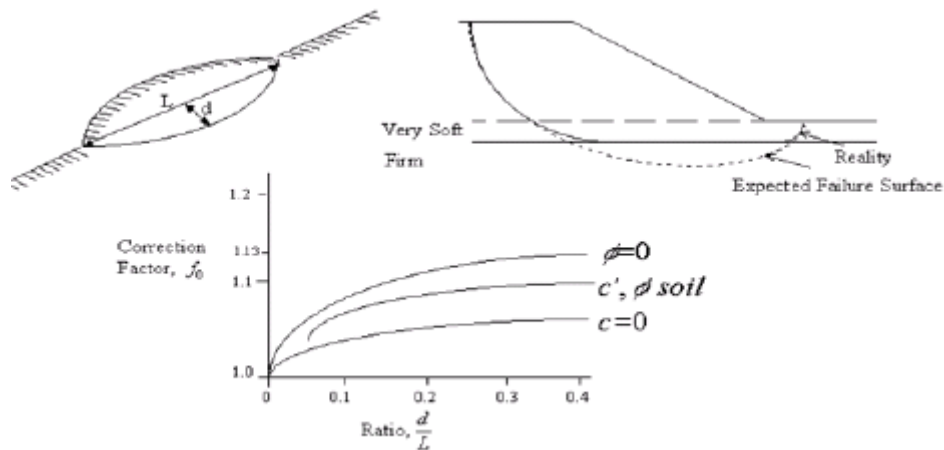


Fig 36: Variation of the correction factor according to depth and length of the fracture surface. [61]

There is a whole series of limit equilibrium procedures that have been developed to analyze the static stability of slopes. Homogeneous slopes are usually analyzed by methods presented previously (Bishop Simplified 1954; Janbu 1956), which assume the circular fracture surfaces. When soil conditions are not homogeneous, the fracture surfaces are likely to be non-circular. In these cases, it is preferable to use methods like Morgenstern Price (1965), Spencer (1967). [67]

There is also Sarma's method (1973, 1979), where he developed a different approach to determine the safety factor of a slope and which satisfies all the equilibrium conditions limit.

III-4-4 Morgenstern and Price Method (1965)

Morgenstern and Price define a function giving the inclination of the inter-unit forces, this method introduces an arbitrary mathematical function to represent the variation of the direction of the forces between the units:

$$\tan\theta_i = \frac{X}{E} = \lambda \cdot f(x'_i) \quad \text{IV-14}$$

Where:

θ_i : is the angle formed by the resultant and the horizontal, it varies systematically from one slice to another along the sliding surface;

λ : is a constant that must be evaluated for the calculation of the safety factor;

$f(x'_i)$: is the function of variation in relation to the distance along the sliding surface;

x'_i : is the linear normalization of the xi coordinates, with the values of the two ends of the fracture surface equal to zero and π .

This method satisfies all the static equilibrium conditions for each slice, as well as the equilibrium of moments and the equilibrium of forces in the horizontal direction, for the whole mass that slides along a circular or non-circular fracture surface (Morgenstern, N. R. & Price, V. E. 1965).

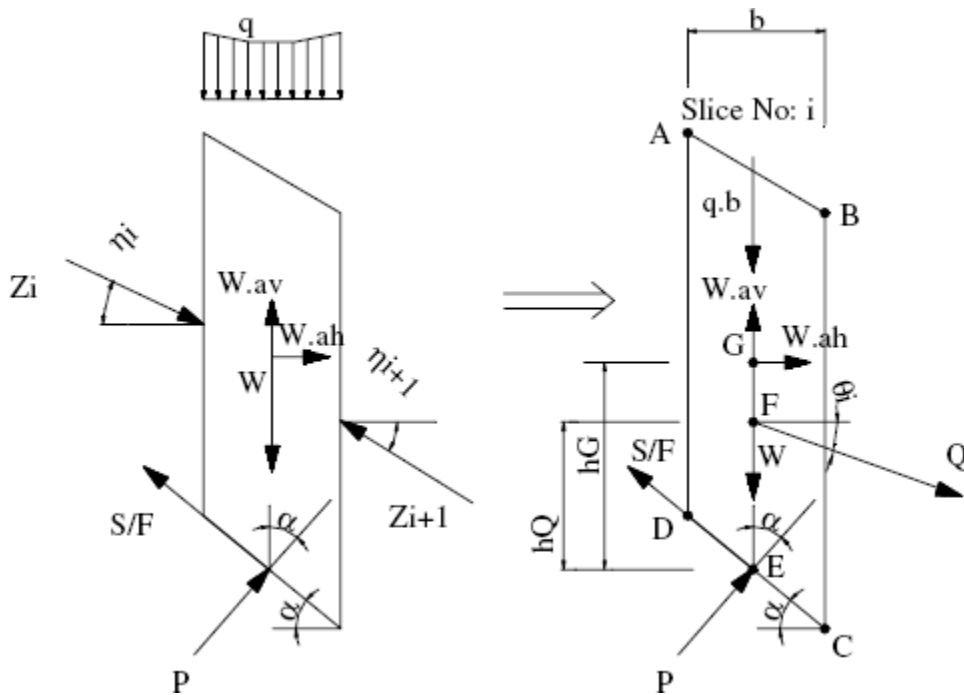


Fig 37: Representation of forces on a slice using the simplified method of Morgenstern and Price. [72]

IV-4-5 The differences between the methods

The following tables summarize the different principles of the different methods:

Table IV-1: Consideration of the balance of forces and moments according to the different methods. [61]

Method	Balance of moments	Balance of forces
Fellenius(ordinary)	Yes	No
Bishop	Yes	No
Janbu	No	Yes
Morgenstern-Price	Yes	Yes

Table IV-2: Consideration of the vertical and horizontal inter-slice forces according to the different methods. [61]

Method	Inter-slice forces vertical (E)	Inter slice forces horizontal (X)
Fellenius (ordinary)	No	No
Bishop	Yes	No
Janbu	Yes	No
Morgenstern-Price	Yes	Yes

IV-5- The finite element method (FEM)

The finite element method is a numerical calculation method which presents a character more physical than abstract; it was invented more by engineers than by mathematicians.

This method was applied for the first time in problems related to the analysis of constraints and since then it has been extended to other problems related to the continuum.

The FEM represents a modality of obtaining a numerical solution corresponding to a specific problem. This method does not offer a formula for a certain solution and does not solve a class of problems. FEM is an approximate method unless a certain problem can be extremely simple thus leading to an exact formula still valid. (The software used in our study is roscience which works based on the MEF). [68;69;70]

IV-5-1- Principle

A non-sophisticated description of the MEF could be defined in the following form:

The structure to be analyzed is divided into several elements (small parts such as those of a jigsaw).

These elements are then reconnected through nodes (these nodes are thumbtacks that keep the elements in a unitary whole).

The behavior of each element is described by a set of algebraic equations.

In stress analysis these equations are not equilibrium equations.

If the variation of displacement or of the stress are negligible along the z axis (the direction normal to the analysis plane) we consider a plane problem.

If displacements or stresses can vary in all directions x, y and z, the structure in question can be called a “3D solid”. [68;69;70]

IV-5-2-Discretization

FEM has developed a series of finite element types:

One-dimensional finite elements.

Two-dimensional finite elements.

Three-dimensional finite elements (solid blocks).

IV-5-3- Behavioral models used in the MEF

The elastoplastic behavior.

The linear elastic model.

The Mohr-Coulomb model:

The Mohr-Coulomb model presents a perfectly plastic elastic behavior without hardening. It has a great use in geotechnics given the results obtained in the calculations. [69]

The model requires the determination of five parameters:

1. Young's modulus E (KPa).
2. Poisson's ratio ν (unitless).
3. Cohesion C (KPa).
4. The angle of internal friction ϕ ($^\circ$).
5. The dilatancy angle ψ ($^\circ$).

IV-5-4- Calculation of the safety factor in the MEF

The reduction of the mechanical characteristics (ϕ -c reduction) is an option available in which makes it possible to calculate safety factors, the characteristics $\tan\phi$ and C are gradually reduced until rupture is achieved. [69]

$$\sum Msf = \frac{\tan \phi_{input}}{\tan \phi_{reduced}} = \frac{C_{input}}{C_{reduced}} = \frac{\text{resistance available}}{\text{Tear resistant}} \quad \text{IV-15}$$

IV-6- Abacus method (Hoek's abacus)

The principle of this method consists in estimating the safety factor according to several parameters: the height of the step (Hg) and the angle of inclination (α) which represent slope parameters; the density (γ), the cohesion (C) and the angle of friction internal (ϕ) which both represent the parameters of the material to be studied.

Several authors have proposed their own abacus, we distinguish: the abacus of Hoek, of Fellinius, from Bishop-Morgenstern (1960) and from Morgenstern (1963).

This method, established by Hoek, is used to calculate the safety factor Fs. To determine Fs, it suffices to know the function of the slope angle (X) and the function of the step height (Y). The point of intersection of the latter allows us to determine the corresponding safety factor. [53]

Where functions X and Y are defined by:

$$X = \alpha - (1.2 * \phi) \quad \text{IV-16}$$

$$Y = \frac{\gamma * HG}{C} \quad \text{IV-17}$$

Or :

α = slope angle ($^\circ$).

ϕ = angle of internal friction ($^{\circ}$).

γ = rock density (KN/m³).

Hg = step height (m).

C = rock cohesion (KN).

The Hoek chart also makes it possible to determine the reciprocal functions of the safety factor, I.e. to determine the critical height of the steps and the critical angle of inclination of the slope by function of a critical safety factor.[71]

Fig 29, illustrates the Hoek chart and the X and Y functions used to determine the factor of safety (Fs):

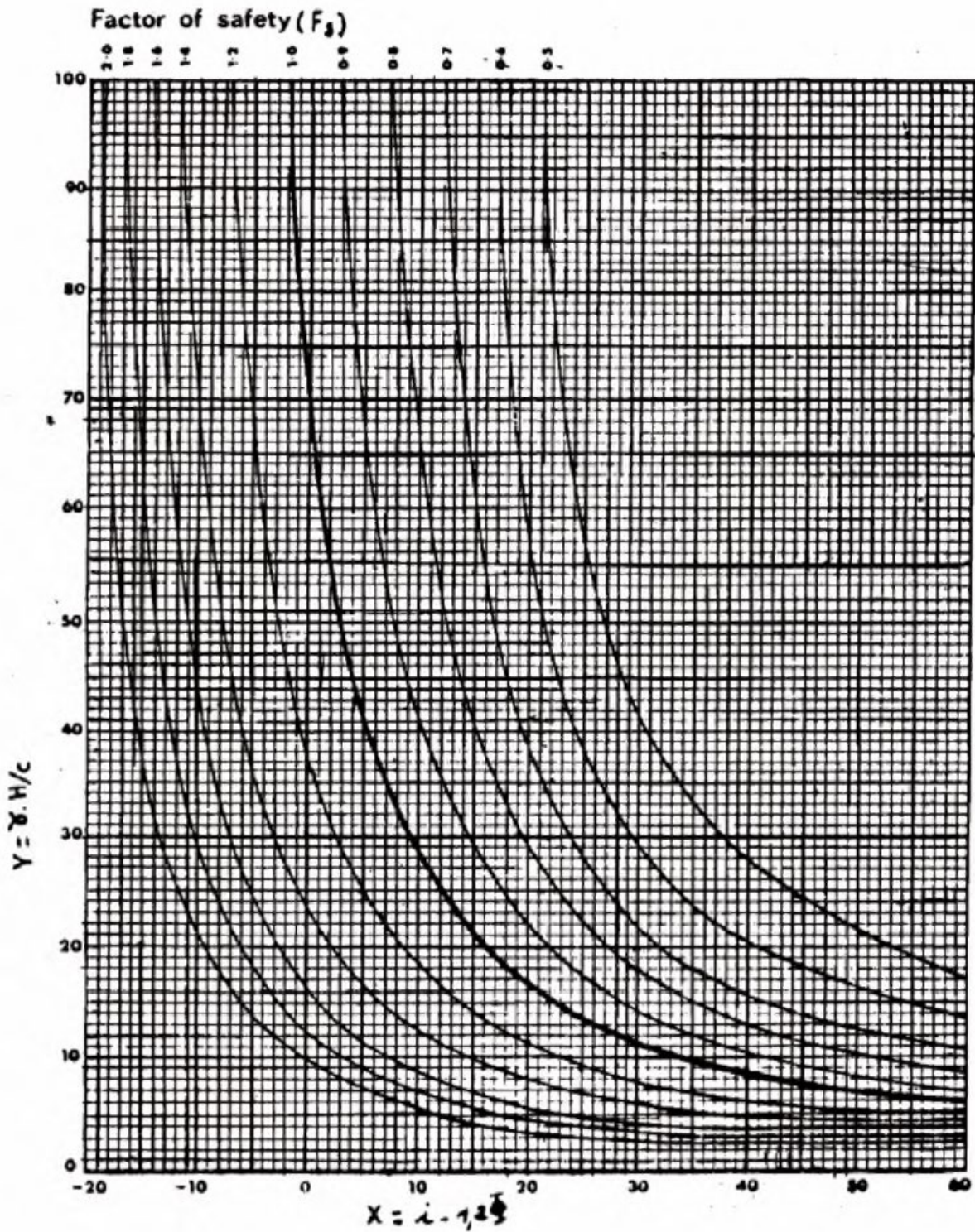


Fig 38: Hoek chart for calculating the safety factor (F_s). [71]

IV-7 Conclusion

The finite element method (FEM) and the limit equilibrium method are two commonly used approaches for analyzing the stability of slopes and structures in geotechnical engineering.

The finite element method is a numerical method that discretizes the slope or structure into small elements and solves the governing equations to determine the stress and deformation distribution. It is a powerful tool for analyzing complex geometries and heterogeneous materials. FEM can provide detailed information on stress distribution, displacement, and failure mechanisms. However, it requires extensive input data and expertise in model calibration, and the computational cost can be significant.

On the other hand, the limit equilibrium method is a simplified approach based on the assumption of equilibrium between driving forces (e.g., gravity) and resisting forces (e.g., shear strength). It involves dividing the slope into individual slices and analyzing the forces acting on each slice. The safety factor, which is the ratio of resisting forces to driving forces, is calculated to assess the stability of the slope. The limit equilibrium method is relatively easy to implement, requires fewer input parameters, and provides a conservative estimate of stability. It is commonly used for preliminary slope stability assessments and design purposes.

CHAPTER

V

V- Introduction

Numerical analysis plays a crucial role in assessing and predicting the stability of mines. It involves using computer-based models and simulations to analyze various factors and conditions affecting the stability of underground or open-pit mines. Here are some key aspects of numerical analysis in mine stability:

Geotechnical Modeling: Numerical analysis starts with developing a geotechnical model that represents the geological and geotechnical conditions of the mine. This includes defining rock properties, structural features, and groundwater conditions. The model can be based on geological mapping, geophysical surveys, and laboratory testing.

Boundary Conditions: The numerical analysis requires defining appropriate boundary conditions, such as stress conditions, displacement constraints, and groundwater flow boundaries. These boundary conditions are essential for accurate modeling of the mine's stability response.

Finite Element/Discrete Element Method: Finite Element Method (FEM) and Discrete Element Method (DEM) are commonly used numerical techniques for mine stability analysis. FEM models the mine as a continuum, whereas DEM considers the individual behavior of discrete rock blocks. Both methods have their strengths and limitations, and the choice depends on the specific mine geometry and stability concerns.

Excavation and Support Simulation: Numerical analysis allows simulating the excavation process and the installation of support systems within the mine. This helps in evaluating the stability of excavations, assessing stress redistribution, and optimizing the design and placement of support structures such as bolts, shotcrete, and ground reinforcement.

Stress Analysis: Numerical models can simulate stress distribution within the rock mass, allowing engineers to analyze potential failure mechanisms, identify critical areas, and assess the overall stability of the mine. This information is crucial for determining appropriate support measures and monitoring systems.

Sensitivity Analysis and Risk Assessment: Numerical models enable sensitivity analysis, where various parameters and scenarios can be tested to assess their influence on mine stability. It helps in identifying critical factors, evaluating uncertainties, and conducting risk assessments to minimize potential hazards and optimize mine planning.

Monitoring and Validation: Numerical analysis can be used to validate monitoring data obtained from instruments installed in the mine. By comparing model predictions with actual measurements, engineers can refine the models and improve their accuracy over time.

Numerical analysis provides valuable insights into mine stability, aiding in the design of safe excavation layouts, support systems, and risk mitigation strategies. It helps mine engineers and geotechnical specialists make informed decisions to ensure the stability and safety of mining operations.

V-1 The creating the geological section

Using Surfer 16 software to create a geological cross-section of the Gara Djebilet region from borehole logs is a common and effective approach. Here is a general procedure to guide you through the creation of the geological section:

Data collection: Gather all available borehole logs for the Gara Djebilet area and Data preparation: Ensure that the borehole log data is compatible with Surfer 16. Generally, the data is supplied in the form of table files. Check whether the data requires any modifications or additional processing in order to be used in Surfer 16.

Importing data into Surfer 16: Launch Surfer 16 and import the survey log data into the software. You can generally import the data using file formats such as CSV, TXT, DAT, etc. Creating the geological section: Once the data has been imported, you can start creating the geological section in Surfer 16. Use the software's tools and functions to trace the various sounding logs along a cross-section line representing the desired geological section.

To enhance the visual representation of the geological section. You can adjust scales, add legends, annotations and titles, and choose the appropriate colours and line styles for each sounding log.

Identify variations in lithology, contacts between geological formations and other relevant features. This can help to understand the geology of the Gara Djebilet region and identify potential areas of interest for mining.

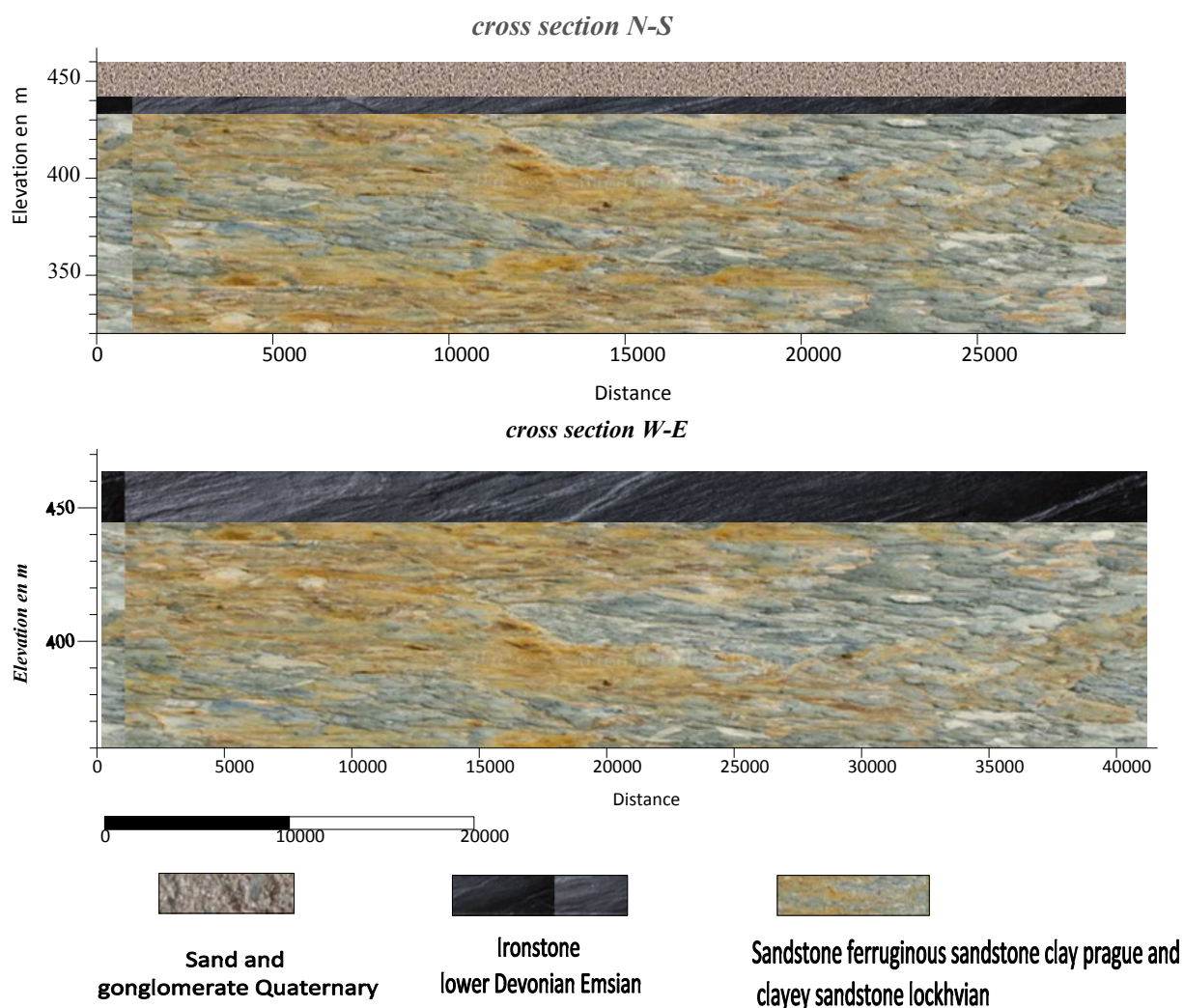


Fig 39: Cross section geological

V-2 Creating geometric models

Creating geometric models for a mine involves collecting topographical and geological data on the site. The geometry of the mine, including ore layers and geological structures. It is interesting to note that GEO-SLOPE and PLAXIS 8.2 software are being considered for the creation of geometric models and to ensure the stability of iron ore mining at Gara Djebilet.

GEO-SLOPE is a geotechnical software package that is widely used to analyse slopes, landslides and geotechnical stability. It is used to model and analyse the behaviour of soils and rocks, taking into account applied forces, hydrogeological conditions and material properties. In the mining context, GEO-SLOPE can be used to assess the stability of mine walls, slopes and excavations.

PLAXIS 8.2 is an advanced geotechnical software package for modelling and analysing the behaviour of soils and geotechnical structures under static and dynamic loads. It is often used to analyse the stability of underground excavations, foundations and complex geotechnical structures. In the case of iron ore mining, PLAXIS 8.2 can be used to assess the stability of tunnels, shafts and underground excavations associated with mining.

Table V-1: Geotechnical parameters of the layers

Layers	γh (kN/m ³)	Young's Module (GPa)	Poisson ratio	C(kPa)	ϕ (°)
Ironstone	37	135	0,27	437	36
Clayey sandstone	29.8	10	0,31	230	33,82
Sand	19	0,5	0,3	0,001	30

V-2-1 By geo-slope code

Calculation of the safety factor using the Morgenstern-Price method (According to Mohr-Coulomb's law of behavior)

V-2-1-A- Geometry model

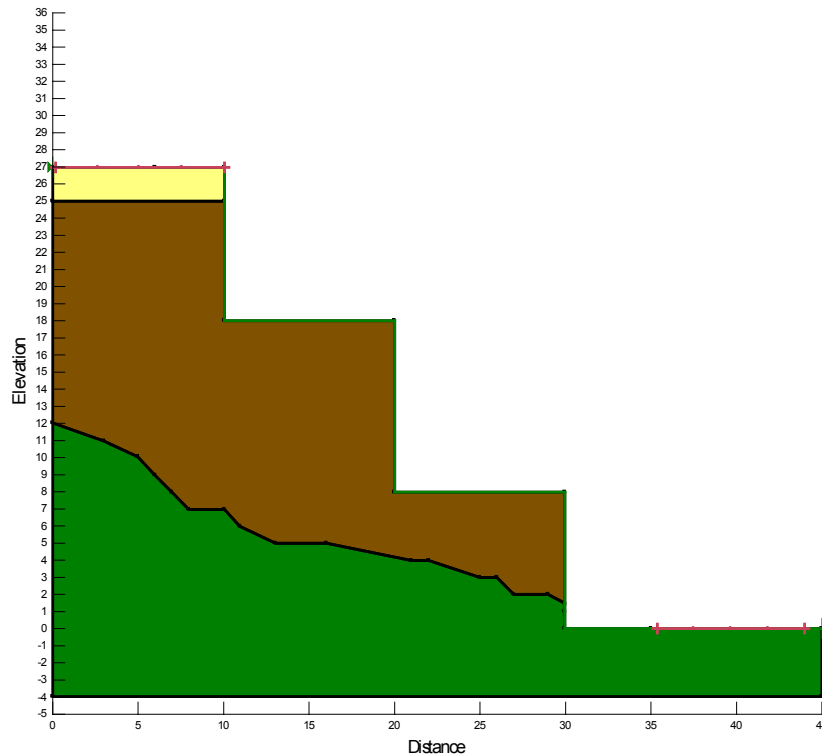


Fig 40: Geometry of model 1

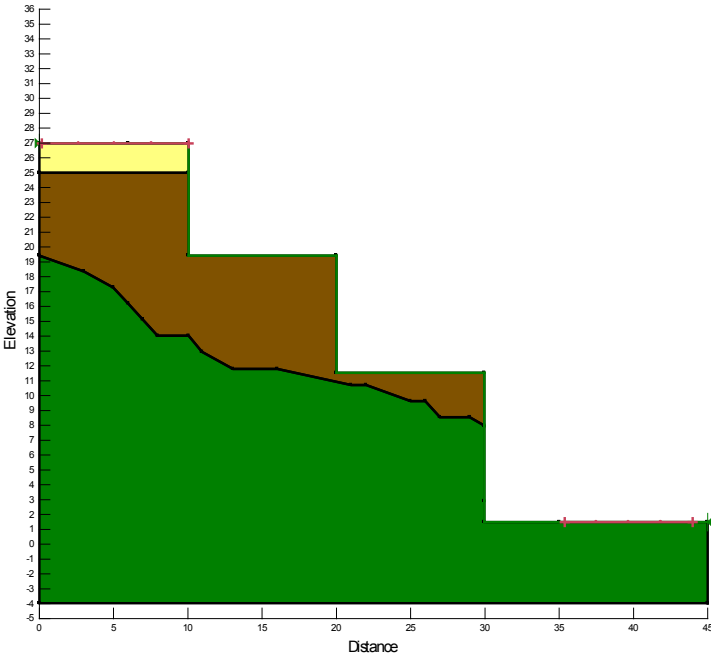


Fig 41: Geometry of model 2

V-2-1-B Calculation

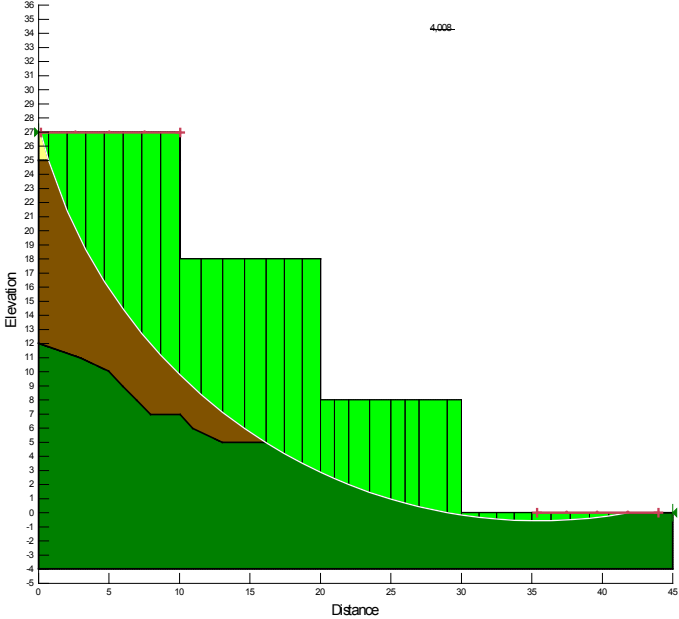


Fig 42: Failure area and value of F_s model 1

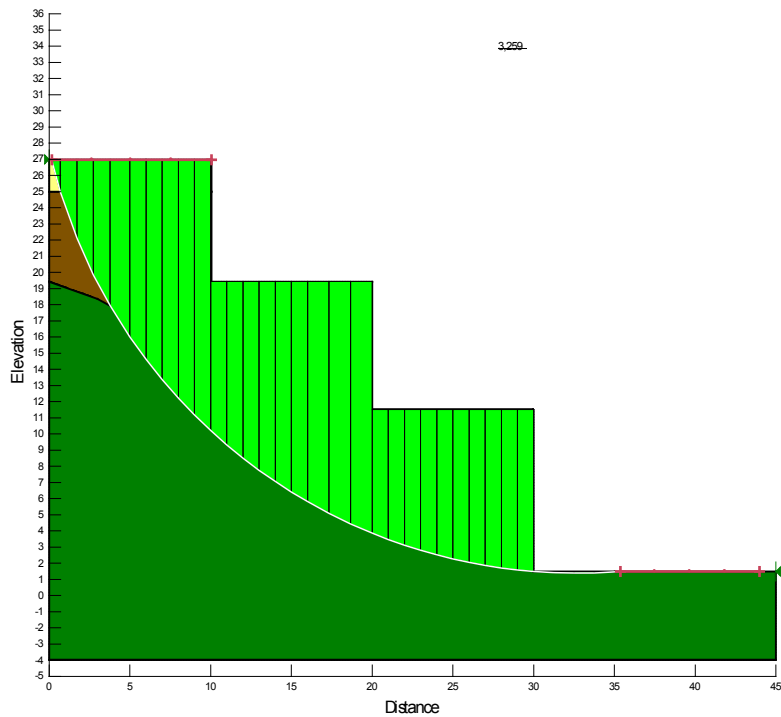


Fig 43: Failure area and value of F_s model 2

Interpretation

The F_s values varied between 4,008 and 3,259 the model 01 and 02 are stable ($F_s > 1$)

We seem to be talking about using Geo-Slope geotechnical software to apply the Mohr-Coulomb limit equilibrium method to assess the stability of a geotechnical slope. In this method, the geometry of the model is used to calculate the safety factor values.

In our case, we indicate that the safety factor values obtained using Geo-Slope are greater than 1.5. This means that the slopes analysed are considered stable with a comfortable safety margin, as they have safety factors higher than the minimum value of 1.5. A higher safety factor generally indicates greater slope stability.

It should be noted that the interpretation of the results and the choice of safety factor values depend on the specific context of the project, the acceptable risks and the applicable design standards. It is important to consult a qualified geotechnical engineer to analyse and interpret slope stability results in order to make informed decisions for the design and construction of geotechnical works.

V-2-2 By plaxis 8.2 Code

V-2-2-A Geometry model

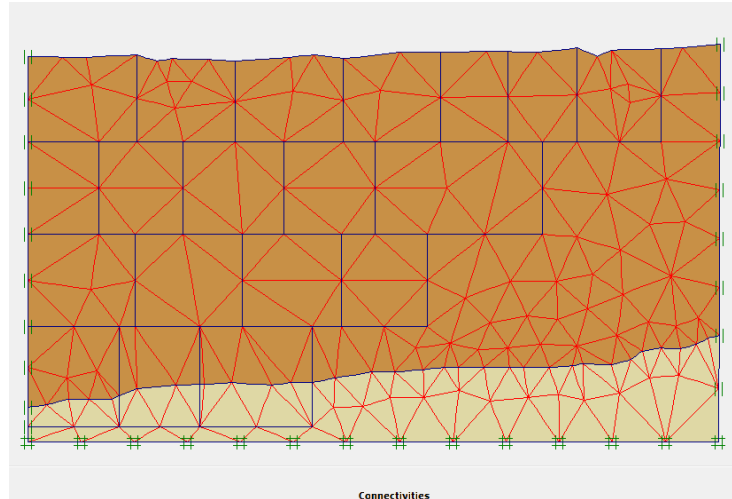


Fig 44: Model geometry (code plaxis 8.2)

V-2-2-B Calculation and output

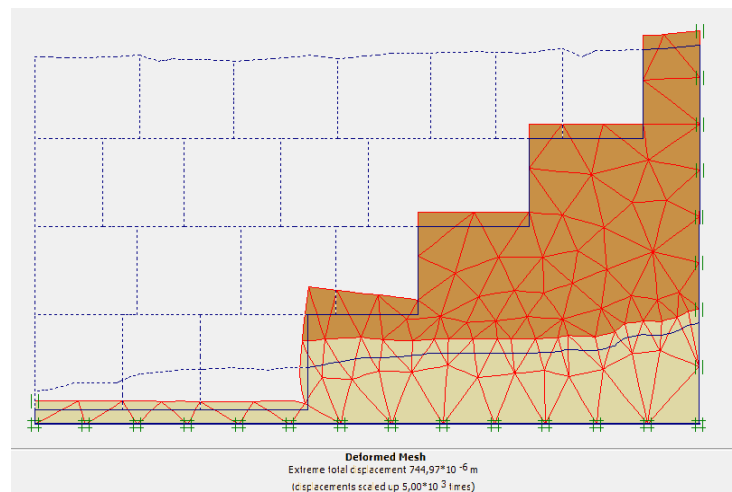


Fig 45 : Displacement total

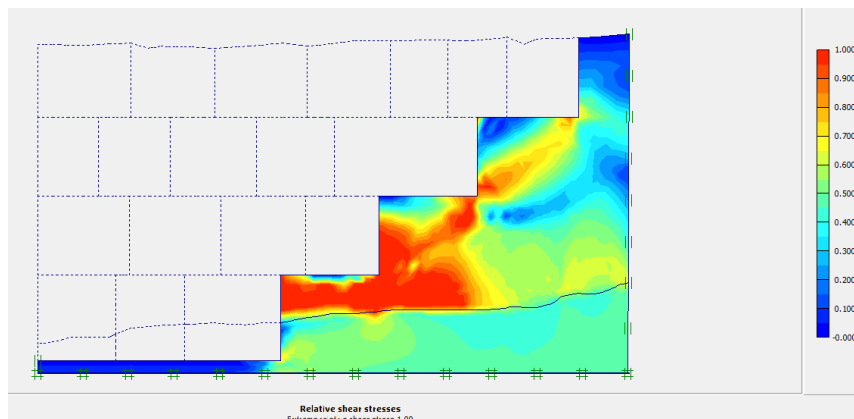


Fig 46 : Relative shear stresses

Chapter V Numerical analysis of the mine stability

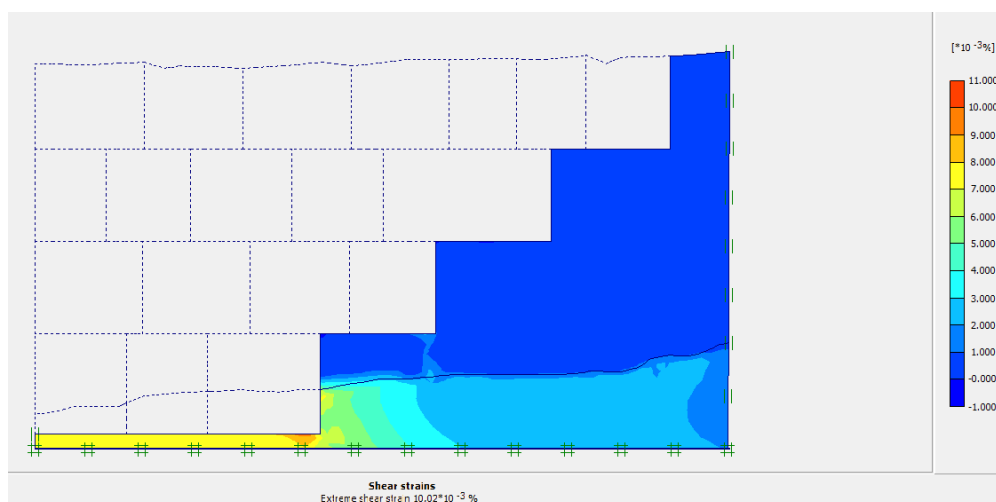


Fig 47 : Shear-strains

PLAXIS - Finite Element Code for Soil and Rock Analyses			
Project description : model gara 1	PLAXIS 8.0		
User name : Koxhiyoki Kabuto, Japan			
Project name : model gara 1	Date : 08/06/2023		
Output : Calculation information			Step : 589 Page : 1
Step Info			
Step 589 of 589 PLASTIC STEP	Incremental Multipliers	0,500 0,000	
Prescribed displacements			
Load system A	Mdisp: 0,000	Σ-Mdisp: 1,000	
Load system B	MloadA: 0,000	Σ-MloadA: 1,000	
Soil weight	MloadB: 0,000	Σ-MloadB: 1,000	
Acceleration	Mweight: 0,000	Σ-Mweight: 1,000	
Strength reduction factor	Maccel: 0,000	Σ-Maccel: 0,000	
Time	Msf: 0,000	Σ-Msf: 2,241	
	Increment: 0,000	End time: 0,000	
Staged construction			
Active proportion total area	Marea : 0,000	ΣMarea : 0,618	
Active proportion of stage	Mstage : 0,000	ΣMstage : 0,000	

Fig 48: Value of the safety factor before exploitation

Chapter V Numerical analysis of the mine stability

PLAXIS - Finite Element Code for Soil and Rock Analyses			
Project description	: model gara 1		PLAXIS 8.0
User name	: Koxhiyoki Kabuto, Japan		
Project name	: model gara 1		Date : 08/08/2023
Output	: Calculation information		Step : 389 Page : 1
Step Info			
Step 389 of 500 PLASTIC STEP	Incremental Multipliers	0,500 0,001	
Prescribed displacements	Mdisp: 0,000	Σ-Mdisp: 1,000	
Load system A	MloadA: 0,000	Σ-MloadA: 1,000	
Load system B	MloadB: 0,000	Σ-MloadB: 1,000	
Soil weight	Mweight: 0,000	Σ-Mweight: 1,000	
Acceleration	Maccel: 0,000	Σ-Maccel: 0,000	
Strenght reduction factor	Msf: -0,001	Σ-Msf: 0,936	
Time	Increment: 0,000	End time: 0,000	
Staged construction			
Active proportion total area	Marea : 0,000	ΣMarea : 0,374	
Active proportion of stage	Mstage : 0,000	ΣMstage : 0,000	

Fig 49: Value of the safety factor After exploitation

V-3 Results and conclusion

Following the numerical analysis using the elaborated cross section along many sectors in the studied area, and using geological logs description make it possible to provide a representative geological cross sections that describe the in-situ state of the iron mine.

The cross section allows us to make a different predictive model of different geometry respecting the exploitation procedure. The results lead to conclude that:

The main layers composed the mine are sand and conglomerate, ironstone, and the lower layer is essentially composed of sandstone and clayey sandstone.

Each geotechnical parameters obtained from samples collected and tested at the geotechnical laboratory of the mining institute, also compared to those effectuated by the society has been used to obtain the geotechnical cross section to elaborate numerical models analyzed using Plaxis and Geo-slope program.

Different scenarios and optimizations allows determining the critical state of the open pit mine stability where the exploitation reach the base layer of sandstone with a factor of safety less than 1. All the senarios otherwise present a stable slopes with safety factors greater than 2.

General

Conclusion

General conclusion

General conclusion

The Gara Djebilet deposit, situated approximately 140 km south-east of Tindouf in south-west Algeria, near the border with Western Sahara, holds significant geological importance as a major iron ore deposit. Geologically, it is located within the Hoggar region, a part of the Saharan Atlas Mountains. The deposit primarily comprises sedimentary rocks, including sandstone, limestone, and shale, which host the valuable iron minerals. The region's geographic characteristics highlight its desert environment, occupying an arid zone of the Sahara marked by hot climatic conditions and limited rainfall. Vast stretches of sand dunes and rocky plateaux form the distinctive landscape of the Gara Djebilet region. Structurally, the Gara Djebilet deposit lies within an area of complex geological formations resulting from past tectonic activity. The region has experienced tectonic movements such as folding, faulting, and fracturing, which have played a crucial role in the formation of the iron ore deposit. It is worth emphasizing that comprehensive geological studies are commonly undertaken to gain a better understanding of the deposit's geology, geography, and structure. These studies are instrumental in determining the distribution of iron minerals, configuring the deposit, and selecting the most appropriate mining methods.

In this chapter, several semi-empirical classification methods for rock masses, including Rock Quality Designation (RQD), Rock Mass Rating (RMR), and Stress Measurement Ratio (SMR), have been investigated and deemed suitable. These classification methods involve both descriptive and quantitative assessments, enabling the evaluation of rock mass quality.

Regarding the specific iron rock mass, it can be concluded that the geological base layer of the iron ore consists of alternating clayey sandstones and clays at certain levels, with conglomerate and quaternary deposits covering the area. These rock formations are classified as high-quality rocks.

In geotechnical engineering, two commonly used approaches for analyzing the stability of slopes and structures are the finite element method (FEM) and the limit equilibrium method. The finite element method employs numerical techniques to discretize the slope or structure into smaller elements and solves the governing equations to determine stress and

General conclusion

deformation distributions. It is a powerful tool capable of analyzing complex geometries and heterogeneous materials, providing detailed information on stress distribution, displacement, and failure mechanisms. However, its implementation requires extensive input data, model calibration expertise, and can be computationally intensive.

On the other hand, the limit equilibrium method offers a simplified approach based on the assumption of equilibrium between driving forces, such as gravity, and resisting forces, such as shear strength. The method involves dividing the slope into individual slices and analyzing the forces acting on each slice to calculate the safety factor, which assesses slope stability. The limit equilibrium method is relatively straightforward to implement, requires fewer input parameters, and provides a conservative estimate of stability. It is commonly employed for preliminary slope stability assessments and design purposes.

Geotechnical laboratory tests are essential for analyzing and obtaining geotechnical parameters of rock masses. Tests such as the Uniaxial Compressive Strength (UCS) Test determine the maximum compressive strength of rock samples, applying axial load until failure occurs. This test helps assess the rock's ability to withstand compressive stresses. Additionally, the Point Load Index (PLI) Test serves as an indirect measure of rock strength when intact rock cores are unavailable. By applying load to a rock specimen using a specialized apparatus, the peak load is recorded, allowing estimation of the uniaxial compressive strength and the rock mass rating (RMR).

These laboratory tests, combined with in-situ testing and field observations, significantly contribute to the characterization of geotechnical properties in rock masses. The parameters obtained from these tests are vital for rock engineering projects and slope stability analysis, as they enhance understanding of the behavior.

Bibliography

Bibliography

- [1] Bersi M et al ; 2010. Aerogravity and remote sensing observations of an iron deposit in Gara Djebilet, southwestern Algeria. *Journal of African Earth Sciences*, 116,134-150.
- [2] Kouche M; 2007. Application of fission traces dating to the analysis of thermicity of basins with oil potential. Example of the Sbaâ basin and the Ahnet-Nord basin (western Saharan platform, Algeria), Doctoral thesis, University of Bordeaux 1
- [3] Hafsaoui cai; March 2018. Environmental, Social and Economic Impact Assessment (EIESE) project for the exploitation of an iron ore deposit.
- [4]Boutiche Ahmed & all ; Oct 2016. Notice explicative associe à la carte géologique Gisement Gara Djebilet (Gara Ouest).
- [5] International Journal of Minerals and Metallurgy; April 2015, issue 4 p34.
- [6]Schlumberger and Sonatrach; 2007. Well Evaluation Conference Algeria. Ed. Schlumberger , 63-68 p.
- [7]Fabre.J; 2005. Geology of western and central sahara. Royal museum for central Africa, Tervuren.
- [8]Mathron.G; 1955. The Gara Djebilet iron deposit Algerian Mining Research Bureau (BRMA); 52-66.
- [9]<https://dz.kompass.com/c/feraal-spa-l%C2%92entreprise-nationale-du-fer-et-de-l%C2%92acier/dz278973/>
- [10]Schlumberger and Sonatrach, 2007. Well Evaluation Conference Algeria. Éd. Schlumberger, pp.63-68.
- [11]Rémi leprete; 2015. Phanerozoic evolution of the West African Craton and its North and West borders-Doctoral thesis-Paris-Sud University/DOCTORAL SCHOOL: MIPEGE 534 -UMR 8148 GEOPS /Sciences de l'Univers/.
- [12]Bessoles. B; 1977. Geology of Africa the West African craton. *Memoirs BRGM*, 88 Paris.
- [13]Chabou-M.C; 2001. Petrographic and geochemical study of magmatism Western Mesozoic of the Saharan platform, Magister thesis, Ecole Nationale Polytechnic, Algiers, 181p
- [14]Selley.RC; 1997. The basins of North-West Africa: structural evolution. In *Sedimentary basins of the world Vol. 3*, pp. 17-26.

Bibliography References

- [15] Gevin.P; 1960. Study and geological reconnaissance on the Yetti-Eglab crystalline axis and its sedimentary border"; first part: sedimentary border. Publ. Servcart Geol. Algeria. Bull no. 23, 328 p
- [16] Boudjemaa.A; 1987. Structural evolution of the "Triassic" oil basin of the Sahara north-eastern (Algeria).
- [17] Yaichi.A & all; 2016. Litho-stratigraphic study and sedimentology of the Lower Devonian - Middle Devonian D'Oued Talha -Tindouf .
- [18] Fabre.J; 2005. Geology of Western and Central Sahara. Royal Museum for Central Africa, Tervuren.
- [19] Bersi, M; 2016. Aero gravity and remote sensing observations of an iron deposit in Gara Djebilet, southwestern Algeria. Journal of African Earth Science.
- [20] Kettouche D;2009. Impact of the Hercynian structure on the oil system of the Tindouf basin.
- [21] Medaouri M; 2004. Structural study of the Ougarta-anti-atlas junction, region of Zemoul-Adhin filou (Western Saharan platform, Algeria).
- [22] According to DRE Tindouf; 2012. The different aquifers that concern the Tindouf basin are from bottom to top
- [23] DRE TDF; 2012. Schematic map showing the distribution of the different aquifers in the Tindouf basin.
- [24] Sambaoui Salah; 2020. Hydro-Environmental Study Applied in Hydrogeology: Case of Oum el Assel, University Center of Tindouf
- [25] <https://www.climatsetvoyages.com/climat/algerie/tindouf>
- [26] Menasri, Y. 2009. Topic: Seismic Vulnerability Assessment of Existing Buildings Portal structure in reinforced concrete"
- [27] Hafsaoui cei; 2018. Environmental, social and economic impact study project (eiese) for the exploitation of an iron ore deposit initial state of gara djebilet (wilaya of tindouf)
- [28] Bersi M. Saibi H and Chabou M C ; 2016. Aerogravity and remote sensing observations of an iron deposits in Gara Djebilet, southwestern Algeria, Journal of African Earth Sciences, 116, 134 & 150
- [29] Kapinga K; 2019. Contribution of remote sensing in geological mapping: case of the Gara Djebilet region (Tindouf basin, Algeria)

Bibliography References

- [30] Guerrak S; 1988. Geology of the Early Devonian oolitic iron ore of the Gara Djebilet Field, Saharan Platform, Algeria, *Ore Geology Reviews* 03- 333-358 p.
- [31] Chalhoub M; 2006. Contributions of numerical homogenization methods to the classification of fractured rock masses.
- [32] Armatys, M; 2012. Modification of geomechanical classifications for shale rock masses.
- [33] Lecheheb A. Yellas CE & Benzaid.RE ; 2020. Geomechanical characterization and classification of rock masses, located between El Aouana and the Aftis Wilaya of Jijel
- [34] Sadek K , Chaouch I & Kamli O; 2016. Characterization and classification of the rock massif of Djebel de Boukhadra-Tébessa
- [35] Dali Omar H; 2019. Characterization and geomechanical classification of the rock masses of Ait Yahia Moussa (Case study: Penetrating Tizi Ouzou–Bouira PK13-PK15)
- [36] Merrien-Soukatchoff V; 2002. Use of rock mass classifications for the analysis of slope behavior. Presentation of two application cases.
- [37] Palmstrom, A; 2005. Measurements of and correlations between block size and rock quality designation (RQD). *Tunnelling and Underground Space Technology*, 20(4), 362-377.
- [38] Deere. DU & Deere.DW; 1989. Rock Quality Designation (RQD) after Twenty Years. Deere (Don U) Consultant Gaines ville Fl.
- [39] Hamidi.JK, Shahriar.K, Rezai.B & Rostami.J; 2010. Performance prediction of hard rock TBM using Rock Mass Rating (RMR) system. *Tunnelling and Underground Space Technology*, 25(4), 333-345.
- [40] Jalalifar.H, Mojedifar.S & Sahebi.A; 2014. Prediction of rock mass rating using fuzzy logic and multi-variable RMR regression model. *International Journal of Mining Science and Technology*, 24(2), 237-244.
- [41] Rehman.H, Ali.W, Naji.A, M. Kim.J. Abdullah.R. & Yoo HK; 2018. Review of rock-mass rating and tunneling quality index systems for tunnel design: Development, refinement, application and limitation. *Applied sciences*, 8(8), 1250.
- [42] Bairi.A; 1990. Method of quick determination of the angle of slope and the orientation of solar collectors without a sun tracking system. *Solar & wind technology*, 7(2-3), 327-330.

Bibliography References

- [43] Mekki.Y & Zouai.A; 2020. The causes of rock instabilities in the Boukhadra mine, Tébessa, eastern Algeria
- [44] Baba Salah; 2016, "Geotechnical design of open pit mine embankments: the case of the Zouerate hematite quartzite quarry".
- [45] Romana.M. Tomás.R & Serón.JB. 2015. Slope Mass Rating (SMR) geomechanics classification: thirty years review. In 13th ISRM international congress of rock mechanics. OnePetro.
- [46] Romana.M; 1991, September. SMR classification. In 7th ISRM Congress. OnePetro.
- [47] Bouali.A & Zeghdani.A; 2019. Rock instability characterization and stabilization case of the road between Hammam Bni Haroun and el Milia
- [48] Mekki.Y & Zouai.A; 2020. The causes of rock instabilities in the Boukhadra Tébessa mine in eastern Algeria
- [49] Bekkar.H & Laouar.F; 2020. Djebel Onk Mine Instabilities: Causes and Remedies
- [50] Romana.M. 1985. New adjustment ratings for application of Bieniawski classification to slopes. In International Symposium on the Role of Rock Mechanics (pp. 49–53). Zacatecas, Mexico.
- [51] Singh, BRK, Goel. "Rock mass classification: a practical approach in Civil"
- [52] Bieniawski. ZT. 1973. "Engineering classification of jointed rock masses." Trans. S. Afr. Instn. Civil Engrs. **15**(12): 335-344.
- [53] John.A. Hudson and Jhon.P. Harrison. 2000. Engineering Rock Mechanics. Introduction to Principles, Imperial College of Science, Technology and Medicine, University of London-UK, 458 p.
- [54] Collin.F. Fox.R. Makeup.R. Schroeder.Ch. 2010 .Stability of Rock Walls: Landslide of the RN 27 Michelau quarry Technical day, administration of the bridges and roads of Luxembourg; 71 p
- [55] Mohamed Khemissa; 2006. Methods for analyzing stability and techniques for stabilization of slopes. Laboratory for the Development of Geomaterials.
- [56] Jean-Pierre Masekanya. 2008. Slope stability and partial saturation, experimental study and numerical modeling.
- [57] Durville.JL. Heraud.H; 2001. Description of rocks and rock masses C352:Engineering technique, construction treaty; 13 p.

Bibliography References

- [58] Lee.W. Abramson and A. Wiley; 2002. Slope Stability and Stabilization Methods, Second edition, Intersection Publication, Jhon Wiley & Fils, Inc, ISBN 0-471-38493-3 736 p.
- [59] Armando Manuel Sequeira Nunes Antão, 1997. Analysis of the stability of underground structures by a regularized kinematic method.
- [60] Françoise Homand and Pierre Duffaut, 2000. Manual of mechanics of rocks, presses the school of Mines Paris.
- [61] GEO-SLOPE International Ltd. March 2008. Stability Modeling With SLOPE/W 2007 Version an Engineering Methodology - Third Edition,.
- [62] Alonso.E; 1976. Risk Analysis of Slopes and Its Application to Slopes in Canadian Sensitive Clays.
- [63] Soukatchoff.VM; 2007. Course in geotechnics from the National School of Mines in Nancy; 100 p.
- [64] Bustamante.AM; 2010. Study of the seismic stability of three natural embankments in Quebec. 220 p
- [65] Hamidi, M; 1994. Geotechnical study of the stability of the embankments in the Zerga district of the Ouenza mine, 162 p.
- [66] Rahmani.N; 2011. Stochastic methods for calculating slope stability.192 p.
- [67] Terzaghi.BRK, PECK.G & MESRI; 1996. Soil Mechanics in the Practices of Engineering, 3rd John Wiley & Sons- INC, 665p.
- [68] Oudin.H ; 2008. Finite element method.
- [69] Brinkgreve. R.B.J W. Broere; 2016. Plaxis Manuals: Plaxis 2D version 8.2, Delft University of Technology and Plaxis- Netherlands, 18p.
- [70] Ciarlet.P & Luneville.E; 2022. The finite element method: from theory to practice. ISTE Group.
- [71] Hoek F & Brown ET; 1980. Underground Excavations in Rocks.